AD-757 050

EXCITATION AND DEEXCITATION OF VIBRATION IN GASES BY OXYGEN AND NITROGEN ATOMS

Graham Black, et al

Stanford Research Institute

AD757050

Final Report

EXCITATION AND DEEXCITATION OF VIBRATION IN GASES BY OXYGEN AND NITROGEN ATOMS

D D C

MAR 15 1973

B
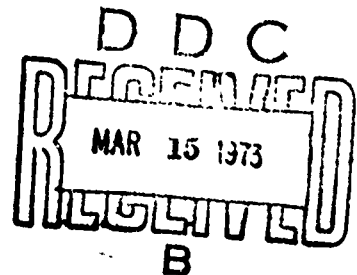
STANFORD RESEARCH INSTITUTE
Menlo Park, California 94025 · U.S.A.
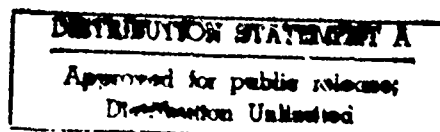
STANFORD RESEARCH INSTITUTE
Menlo Park, California 94025 · U S A

Final Report   *February 16, 1973*

EXCITATION AND DEEXCITATION OF VIBRATION
IN GASES BY OXYGEN AND NITROGEN ATOMS

By: GRAHAM BLACK and DONALD J ECKSTROM

Approved by:

FELIX T SMITH, *Manager*
Molecular Physics

CHARLES J COOK, *Executive Director*
Physical Sciences Division

I

CONTENTS

SYNOPSIS

The earth's upper atmosphere continuously emits infrared radiation. Some of this radiation is powered by the energy stored in vibrationally excited nitrogen that can be produced by a number of exothermic processes. One of these processes is the reaction $NO + N \rightarrow N_2 + O$, in which 3.27 eV is available for vibrational and rotational energy of the N_2 product as well as for kinetic energy.

The first task of the research program was to determine the fraction of the energy appearing in N_2 vibrations by the use of Raman spectroscopy to determine the population of $N_2(v=1)$ that is produced. These measurements established that $25 \pm 3\%$ of the exothermicity of the reaction appears as vibrational energy in the nitrogen and that the $NO + N \rightarrow N_2 + O$ reaction is an important source of vibrationally excited N_2 in the E region. An article describing the measurements has been accepted by the Journal of Chemical Physics and is attached as Appendix A to this report.

Once produced, the vibrationally excited nitrogen is deexcited only by collisions. In the E region, one important quenching mechanism is energy transfer to CO_2, the rate for which is moderately well known. A second important deexcitation mechanism was considered to be V-T energy exchange with $O(^3P)$. At the start of this research program, the rate coefficients for this latter process were only known for translational temperatures far higher than are found in the earth's atmosphere.

Therefore, Task II of our work was to measure this rate down to as low a temperature as possible by the use of a shock tube with ozone as the source of atomic oxygen and the infrared-tracer method to monitor the vibrational energy in the nitrogen. These measurements have established that V-T relaxation of $N_2(v=1)$ by $O(^3P)$ is an efficient process

with a rate varying from 1 atm-μsec at 3000 K to 2 atm-μsec at 1200 K. Our results are in agreement with recent results at lower temperature in an afterglow experiment carried out by McNeal, Whitson, and Cook.[1] In addition, the results show that $O(^3P)$ V-T relaxation plays an important role in determining the vibrational temperature of N_2 in the E region. The results are fully described in an article that has been submitted for presentation and publication in the proceedings of the Ninth International Shock Tube Symposium (Stanford University, July 1973). This article constitutes Appendix B to this report.

In summary, quenching of vibrationally excited nitrogen by atomic oxygen appears to be an important loss process for $N_2(v=1)$ in the lower thermosphere. The use of correct rates for this process results in a large reduction in the expected N_2 vibrational temperature in this region.

LIST OF ILLUSTRATIONS

I INTRODUCTION

In the E region of the earth's atmosphere, a number of exothermic chemical reactions occur that can produce $N_2^\ddagger$, vibrationally excited nitrogen. In the lower E region (below 125 km), a major loss of nitrogen vibrational energy is by energy transfer to CO_2,

$$N_2(v=1) + CO_2 \rightarrow CO_2(\nu_3=1) + N_2 - 18cm^{-1} \quad , \tag{1}$$
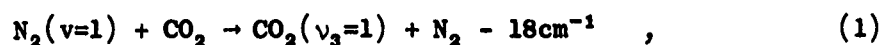
with subsequent radiation in the infrared (principally at 4.3 μ). Processes that excite or deexcite $N_2^\ddagger$ are thus of particular interest in connection with some defense problems concerned with atmospheric infrared measurements.

The main processes that have been considered for producing $N_2^\ddagger$ are:

$$N(^4S) + NO \rightarrow N_2 + O(^3P) + 3.27 \text{ eV} \tag{2}$$

$$O(^1D) + N_2 \rightarrow N_2 + O(^3P) + 1.96 \text{ eV} \tag{3}$$

$$N_2(A^3\Sigma_u^+) + O(^3P) \rightarrow N_2 + O(^3P, {}^1D, {}^1S), \quad \Delta E = 6.2, \ 4.2, \ 2.0 \text{ eV} \tag{4}$$

$$N_2(A^3\Sigma_u^+) + O_2 \rightarrow N_2 + O_2(^3\Sigma, {}^1\Delta, {}^1\Sigma), \quad \Delta E = 6.2, \ 5.2, \ 4.6 \text{ eV} \tag{5}$$

$$e^- + N_2 \rightarrow (N_2^-) \rightarrow N_2^\ddagger + e^- \quad . \tag{6}$$
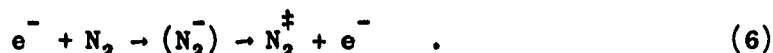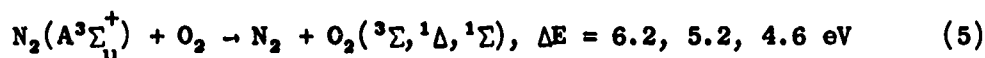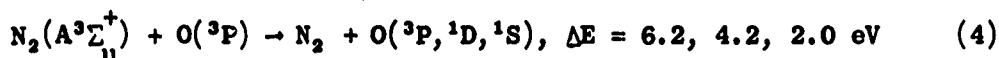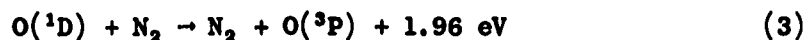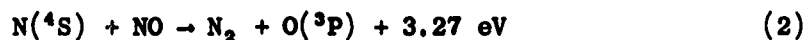
Also, emission of Vegard-Kaplan band radiation by $N_2(A^3\Sigma_u^+)$ in most instances will leave N_2 vibrationally excited. Whereas process (6) is certainly important in auroral conditions, it is not important in the undisturbed E region.

If all these processes were equally effective (as a fraction of the energy available) in producing $N_2^\ddagger$, then, in the E region, process

(3) would produce more $N_2^{\ddagger}$ than process (2), and the latter would produce more than the sum of processes (4) and (5). The first goal of the studies at SRI, therefore, has been to investigate processes (2) and (3).

A second aspect of the atmospheric processes powering emissions through $N_2^{\ddagger}$ concerns the reactions that can quench it in the upper atmosphere. The most important deexcitation mechanisms have been considered to be energy transfer to CO_2 in the lower E region [process (1)]--the rate for which is moderately well known--and diffusion, electron quenching, and V-T energy exchange with $O(^3P)$ in the upper E region and higher. At the time this program was undertaken, rate coefficients for the latter process had been measured only in the temperature range from 3000 to 4500 K.[2] A second goal of our work (Task II) has, therefore, been measurement by shock tube techniques of this rate for temperatures down to 1200 K. Recently, low temperature measurements of the rate of vibrational relaxation of N_2 by $O(^3P)$ have been reported which are many orders of magnitude faster than was anticipated on the basis of theoretical extrapolations of the high temperature results.[1] The intermediate temperature results of this study are therefore of importance to verify the low temperature data and to establish the correct temperature dependence of this rate.

II TASK I: VIBRATIONAL POPULATION MEASUREMENTS

A. Background

One aim of the Task I program has been to determine the efficiency with which processes (2) and (3) produce $N_2^{\ddagger}$.

Measurements of process (2), the N + NO reaction, a decade ago indi-- cated that about 30% of the exothermicity of the reaction appears in $N_2^{\ddagger}$.[3-5] If this is true, and if the efficiency of (3) is as low as was indicated by the theoretical study of E. R. Fisher and E. Bauer[6], then process (2) is much more important than (3) as a source of $N_2^{\ddagger}$. For these reasons, we proposed that a measurement of the efficiency of production of $N_2^{\ddagger}$ in process (2) should be a primary part of the current program.

We had also intended to make measurements of process (2) by the infrared-tracer technique with CO. Unknown to us at the time of writing the proposal, such a program was already under way at Air Force Cambridge Research Laboratories. That program revealed serious problems in inter- pretation when the infrared-tracer technique was applied to process (2). Early in March 1972, the Optical Physics Group of A. T. Stair at AFCRL discussed their findings with us. The problems have also been discussed with Drs. Gilmore and Bauer. In all these discussions, general agreement has been reached that process (2) should be given high priority and that the preferable technique for studying it would be the Raman scattering technique for measuring $N_2^{\ddagger}$. The Raman technique was anticipated to be easier to apply to process (2) than it was in our earlier work on pro- cess (3),[7] both because much higher initial populations of N atoms could be created than was possible with $O(^1D)$ and because of the expectation that about 30% of the reaction energy would appear as vibrations in N_2.[3-5]

Although the main goal of the measurements was to obtain reliable information on the N + NO reaction, it was hoped that the use of the Raman technique for reaction (2) would reveal the causes of the difficulties encountered by others in using the infrared-tracer technique on that reaction. In this way, it should be possible to improve the reliability of the infrared technique.

Last year our measurements were confined to reaction (3)--the quenching of $O(^1D)$ by nitrogen. The vibrationally excited nitrogen was measured by Raman spectroscopy. During the period of that experimental program, a theoretical study by E. R. Fisher and E. Bauer concluded that less than 5% of the $O(^1D)$ electronic energy is channeled into the vibrational levels of N_2.[6] Our experimental findings were inconclusive (see reference 10 of Appendix A) and made further work on this reaction desirable.[7] One objective of the current program was to perform such measurements by using CO as an infrared-emitting tracer of the $N_2^{\ddagger}$. However, because of the difficulties in interpreting the results when the infrared-tracer technique was applied to process (2), its application to process (3) was postponed to some future time.

B. Accomplishments

The reaction

$$N(^4S) + NO \rightarrow N_2(v=n) + O(^3P) \tag{2}$$
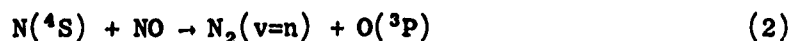
is fast ($\approx 2\times 10^{-11}$ cm^3 $molec^{-1}$ sec^{-1} at room temperature[8,9]) and is sufficiently exothermic (3.27 eV) to produce $N_2^{\ddagger}$ up to n=12. It is expected that the initial vibrational distribution will be rapidly degraded by vibrational exchange collisions of the type

$$N_2(v=n) + N_2(v=0) \rightarrow N_2(v=n') + N_2(v=n-n') \quad , \tag{7}$$

4
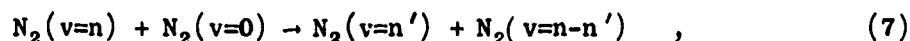
resulting in an increased population of $N_2(v=1)$.[5-7,10-15] Hence a measurement of $N_2(v=1)$ should be sufficient to determine the fraction of the exothermicity of reaction (2) that appears as vibrational energy. Such measurements have been made by observing Raman scattering of 4880 Å Ar^+ laser radiation. The intensity of the Q-branch of the anti-Stokes transition (at 4382 Å) was measured, because the anti-Stokes spectra are free from Raman transitions from the $N_2(v=0)$ level [whereas the Stokes transitions from $N_2(v=1)$ lie in the rotational structure of the Stokes lines from $N_2(v=0)$].

The measurements are fully described in an article that is attached as Appendix A to this report. The conclusion reached was that $25 \pm 3\%$ of the exothermicity of reaction (2) appears as vibrational energy. Of necessity, the use of a rotational Raman spectrum to determine gas temperature is treated only briefly in Appendix A. The purpose of the next section is to describe this measurement in more detail.

C. Temperature Determination from Rotational Raman Spectra

With heating tapes wrapped around the pyrex cell (the first figure of Appendix A), nitrogen at atmospheric pressure was heated to ~ 100 °C. Under these conditions, with a thermocouple close to the focus of the laser beam indicating a gas temperature of 100 °C, the rotational Raman spectrum shown in Fig. 1 was recorded. The series of lines shifted to longer wavelengths of the 4880 Å laser line are called the Stokes lines $(J \rightarrow J + 2)$ and the series of lines shifted to shorter wavelengths are called the anti-Stokes lines $(J + 2 \rightarrow J)$. They are also referred to by some authors as the S branch and O branch, respectively [consistency with international nomenclature would require that both series of lines be called S branches, since $\Delta J = J'-J''$ (J' refers to the upper state and J'' refers to the lower state) is + 2 in both cases].[16] In Fig. 1, the numbering of the lines is the J value of the lower state. The intensity

5
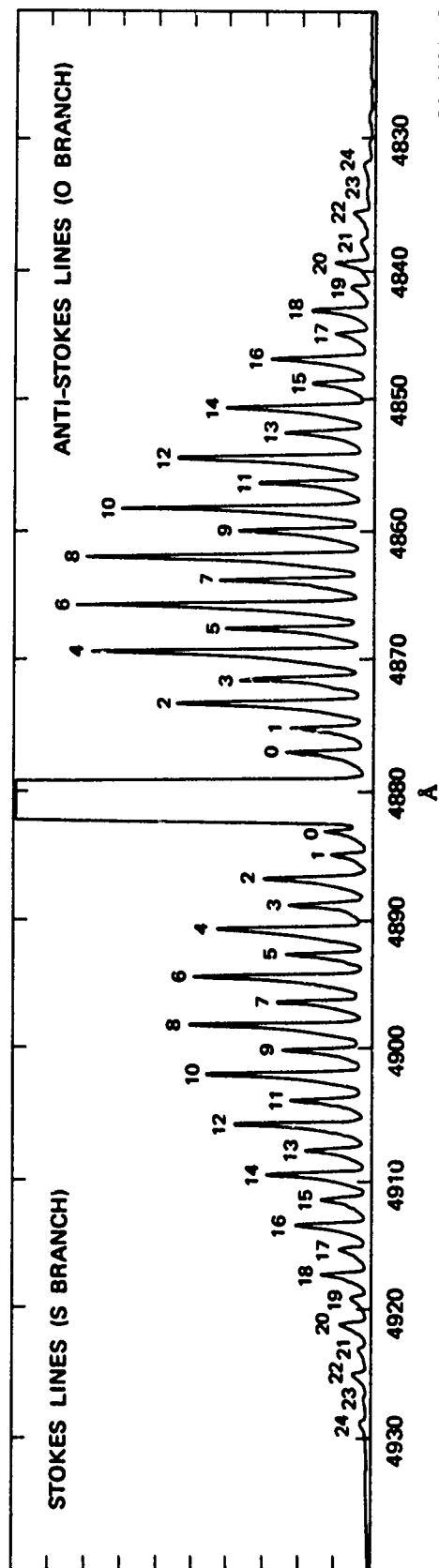
FIGURE 1   ROTATIONAL RAMAN SPECTRUM OF N_2 AT ~ 100°C

SA-1664-4R

6
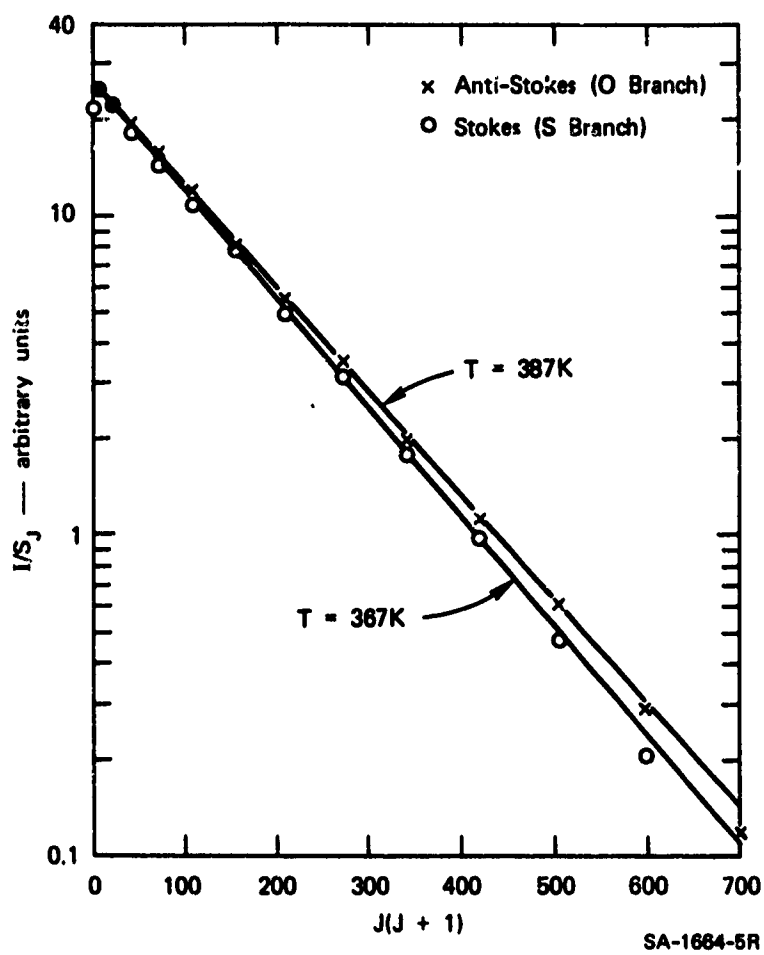
FIGURE 2   TEMPERATURE DETERMINATION FROM THE
ROTATIONAL RAMAN SPECTRUM

In a recently published paper,[18] gas temperatures were deduced by
this same technique from observations of only the Stokes lines without
correcting for the ν^3 dependence of the intensity. The temperatures
deduced were always lower than those measured by a thermocouple. This
agrees with our observations if the ν^3 term is not included. This
shows the importance of including the ν^3 variation if the correct tem-
perature is to be obtained. It should also be stressed that it is im-
perative to determine the gas temperature from both branches of the
rotational Raman spectrum to verify the constancy of the counting ef-
ficiency over the wavelength range of the spectrum.

III TASK II: VIBRATIONAL RELAXATION OF N_2 BY $O(^3P)$

A. Backgrou:.d

The work on Task II, which involves the measurement in a shock tube
of the rate of vibrational relaxation of N_2 by $O(^3P)$ atoms, is a continu-
ation of work carried out in 1970-71 under ARPA Contract DAHCO4-70-C-
0036. The objective has been to determine the relaxation time $p\tau_{N_2-O}$
over the temperature range from approximately 1,000 to greater than
3,000 K for the purpose of comparing the data of Breshears and Bird[2] in
the range from 3,000 to 4,500 K and establishing the temperature-
dependence of the rate for extrapolation to the lower temperatures found
in the upper atmosphere.

The high-temperature shock tube data of Breshears and Bird was ob-
tained using the laser-schlieren technique, in which the density gradi-
ent in the relaxation region behind the shock wave is measured through
its effect on the refractive index of the gas. It was originally in-
tended that the same technique be used at the lower temperatures of
this study; however, it was found that at the lower temperatures the
density gradients are simply too small and disturbances from boundary
layer turbulence are too large for the schlieren or other methods rely-
ing on refractive index changes to be successful. Therefore, efforts
were concentrated on the infrared tracer measurement technique, in which
the radiation from small amounts of CO added to the gas mixture is pro-
portioned to the vibrational energy of the N_2 .

B. Accompl:.shments

The experimental program thus carried out, its interpretation, and
the results are described in full in Appendix B, which is a preprint of

an article submitted for presentation and publication in the proceedings of the Ninth International Shock Tube Symposium to be held at Stanford University in July of 1973. As described in Appendix B, the objective of Task II has been met in full in that the rate of vibrational relaxation of N_2 by $O(^3P)$ has been determined for the temperature range from 1200 to 3000 K. In addition, some limited results for the rate of vibrational relaxation of CO by $O(^3P)$ in the same temperature range have been obtained.

The measured values of $p\tau_{N_2-O}$ range from approximately 1 atm-μsec at 3000 K to 2 atm-μsec at 1200 K, with an uncertainty of $\pm$ 50%. Both the magnitude and the trend of the results are in excellent agreement with the results of Breshears and Bird,[2] as well as with the recent low temperature measurements of McNeal, et al.[1] In marked contrast to theoretical predictions,[3] these combined results establish a slowly varying temperature-dependence for this rate and thus provide a challenge to continuing theoretical efforts to understand this problem. More importantly, however, the combination of the recent low temperature results and the current measurements allows confident specification of the N_2-O rate at the temperatures of the upper atmosphere. Recent studies show that with the use of these new rates,[19-20] the calculated vibrational temperature of N_2 in the E region is much lower than was previoulsy predicted[21] and is in agreement with experiment.

The measured value of $p\tau_{CO_2-O}$, is approximately 0.04 atm-μs over the temperature range from 1200 to 3000 K. This is approximately the same as earlier measurements of $p\tau_{O_2-O}$,[22] and is approximately 25 times more rapid than the N_2-O rate in the same temperature range. This greater rapidity could result from either stronger chemical effects in the CO-O and O_2-O processes or the possibility of atom exchange in these cases.

11

C. Conclusions

At the start of this research program, N_2 vibrational temperatures as high as 3000 K were predicted[21] for the E region. This high vibrational temperature resulted from the balance between efficient production by the reactions

$$N(^4S) + NO \rightarrow N_2(v) + O(^3P) \qquad\qquad (2)$$

$$O(^1D) + N_2 \rightarrow N_2(v) + O(^3P) \qquad\qquad (3)$$
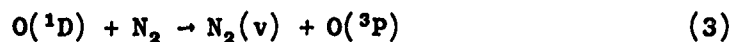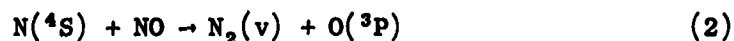
and comparatively inefficient removal by energy transfer to CO_2; that is,

$$N_2(v=1) + CO_2(00^\circ0) \rightarrow N_2(v=0) + CO_2(00^\circ1) \quad . \qquad (1)$$
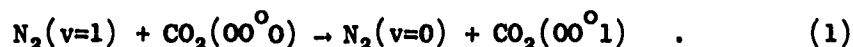
During the course of this contract, McNeal showed that V-T relaxation of $N_2(v=1)$ by $O(^3P)$ was efficient at 300 K and should be considered in determining the vibrational temperature of N_2 in the E region.[1] This was in direct conflict with the theoretical predictions of Fisher and Bauer.[6] The measurements performed under the current contract extend over the temperature range from 1200 to 3000 K, and confirm that relaxation of $N_2(v=1)$ by $O(^3P)$ is indeed efficient. We have also established that process (2) is an efficient source of vibrationally excited nitrogen. The net effect, however, is to expect large reduction in the nitrogen vibrational temperature in the E region (to $\lesssim 1000$ K) and to greatly reduce the sensitivity of the calculated vibrational temperature to the yield of vibrational energy from the $O(^1D) + N_2$ reaction.

12

REFERENCES

1. R. J. McNeal, M. E. Whitson, Jr., and G. R. Cook, Chem. Phys. Letters 16, 507 (1972); Trans. Amer. Geophys. Union (to be published).

2. W. D. Breshears and P. F. Bird, J. Chem. Phys. 48, 4768 (1968).

3. J. E. Morgan, L. F. Phillips, and H. I. Schiff, Disc. Faraday Soc. 33, 118 (1962).

4. L. F. Phillips and H. I. Schiff, J. Chem. Phys. 36, 3283 (1962).

5. J. E. Morgan and H. I. Schiff, Can. J. Chem. 41, 903 (1963).

6. E. R. Fisher and E. Bauer, J. Chem. Phys. 57, 1966 (1972).

7. G. Black and D. J. Eckstrom, "Excitation and Deexcitation of Vibration in N_2 by Oxygen Atoms," Final Report, Contract DAHC04-70-C-0036, Stanford Research Institute, Menlo Park, Calif. (October 1971).

8. J. T. Herron, J. Chem. Phys. 35, 1138, 1961; J. Res. Nat. Bur. Stand. 65A, 411 (1961).

9. L. F. Phillips and H. I. Schiff, J. Chem. Phys. 36, 1509 (1962).

10. J. D. Lambert, "Atomic and Molecular Processes," ed. by D. R. Bates, p. 783, 1962.

11. A. Dalgarno, Planet. Space Sci. 10, 19 (1963).

12. C. C. Rankin and J. C. Light, J. Chem. Phys. 46, 1305 (1967).

13. A. L. Schmeltekopf, F. C. Fehsenfeld, G. I. Selman, and E. E. Ferguson, Planet. Space Sci. 15, 401 (1967).

14. D. Rapp and P. Englander-Golden, J. Chem. Phys. 40, 573 (1964); 40, 3120 (1964).

15. D. Rapp, J. Chem. Phys. 43, 316 (1965).

16. R. S. Mulliken, Phys. Rev. 36, 611 (1930).

17. G. Herzberg, "Molecular Spectra and Molecular Structure. I. Spectra of Diatomic Molecules," p. 134 (D. Van Norstrand Company, Inc., 1950.)

18. R. S. Hickman and L. H. Liang, Rev. Sci. Inst. 43, 796 (1972).

19. E. L. Breig, M. E. Brennan, and R. J. McNeal, J. Geophys. Res (1973), to be published.

13

20. E. Jamshidi, E. R. Fisher, and R. H. Kummler, J. Geophys. Res. (1973), to be published.

21. J. C. G. Walker, Planet Space Sci. 16, 321, (1968); J. C. G. Walker, R. S. Stolarski, and A. F. Nagy, Ann. Geophys. 25, 831, 1969.

22. J. H. Kiefer and R. W. Lutz, Eleventh Symp. (Int..) on Combustion, The Combustion Institute, Pittsburgh, 1967.

APPENDIX A

MEASUREMENTS OF VIBRATIONALLY EXCITED MOLECULES
BY RAMAN SCATTERING.   I.   THE YIELD
OF VIBRATIONALLY EXCITED NITROGEN IN THE REACTION
$$N + NO \rightarrow N_2 + O$$

APPENDIX A

MEASUREMENTS OF VIBRATIONALLY EXCITED MOLECULES BY RAMAN SCATTERING. I. THE YIELD OF VIBRATIONALLY EXCITED NITROGEN IN THE REACTION $N + NO \rightarrow N_2 + O$

Graham Black, Robert L. Sharpless, and Tom G. Slanger
Stanford Research Institute, Menlo Park, California 94025

The reaction of nitrogen atoms with nitric oxide leads to vibrationally excited nitrogen. In the presence of molecular nitrogen, V-V exchange processes rapidly establish a modified distribution for which a measurement of $N_2(v=1)$ is adequate to determine the total vibrational energy yield of the reaction. The measurements of $N_2(v=1)$ have been made by Raman spectroscopy using the intensity of the Q branch of the anti-Stokes line at 4382 Å (using 4880 Å Ar^+ laser radiation). The system sensitivity is determined using heated nitrogen. The measurements have established that 25 ± 3% of the available energy (3.27 eV) appears as vibrational energy and that the vibrationally excited nitrogen is an initial product and does not result from collisions of translationally hot oxygen atoms with nitrogen.

I. INTRODUCTION

Vibrationally excited nitrogen plays a number of important roles in determining the nature of the lower thermosphere--its influence on the ionospheric composition,[1-3] the electron temperature,[4-6] and the energy balance[7] are of special importance.

In the undistrubed E region the two most important processes that produce vibrationally excited nitrogen are[7]

$$O(^1D) + N_2 \rightarrow N_2(v) + O(^3P) \tag{1}$$

and

$$N(^4S) + NO \rightarrow N_2(v) + O(^3P) \quad . \tag{2}$$
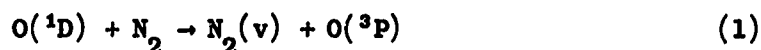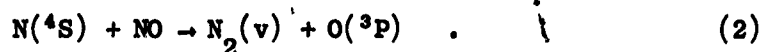
A calculation by Fisher and Bauer[8] indicated that less than 5% of the available energy in reaction (1) (1.96 eV) is expected to channel into the vibrational levels of N_2. An experiment to determine the vibrational yield of reaction (1) was recently carried out in this laboratory,[9] but the results were inconclusive.[10] An efficiency less than 5% makes reaction (1) a minor source of N_2 vibrational energy in the E region.

Measurements of reaction (2) a decade ago by Schiff and coworkers[11-13] indicated that about 30% of the exothermicity of the reaction appears as vibrational energy. Wray[14] has pointed out an alternative interpretation of the earlier measurements, which allows the exothermicity of the reaction to appear as translational energy of the product species--preferentially in the oxygen atom because of its lighter mass. The translationally hot oxygen atoms, under the experimental conditions, would undergo collisions with nitrogen. These collisions would have a high

17

probability of exciting vibrational energy in the nitrogen.[15] The
validity of the earlier measurements can also be questioned on the
grounds that the calorimetric probe used may have responded to energetic
species other than $N_2(v)$.

The experiments to be described below have determined the fraction
of the exothermicity of reaction (2) which appears as vibrational en-
ergy, using Raman scattering as a specific detector of vibrationally
excited nitrogen molecules. The experimental conditions have also been
varied to show that the vibrationally excited nitrogen is a primary
product of reaction (2) and that any production of $N_2(v=1)$ by collisions
of translationally hot oxygen atoms with N_2, if it occurs at all, must
be of minor importance.

II. EXPERIMENTAL

Reaction (2) is fast ($\approx 3 \times 10^{-11}$ cm^3 molec^{-1} sec^{-1} at room tempera-
ture[16]) and is sufficiently exothermic (3.27 eV) to produce $N_2(v)$ up to
v=12. Whatever the intial vibrational distribution, it will be rapidly
degraded by V-V exchange collisions of the type

$$N_2(v=n) + N_2(v=0) \rightarrow N_2(v=n-n') + N_2(v=n') \qquad (3)$$
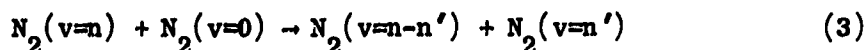
resulting in an increased population of $N_2(v=1)$. (At N_2 pressures of
several torr this will require only a few milliseconds. Loss of vibra-
tional energy by diffusion and wall deactivation is small in this time,
and is taken into account.) Hence a measurement of thermalized $N_2(v=1)$
is sufficient to determine the fraction of the exothermicity of reaction
(2) that appears as vibrational energy.

The principle of the experiment is to make $N_2(vib)$ by reaction (2)
followed by reaction (3), and to monitor the $N_2(v=1)$ concentration by

observing the Raman scattering of 4880 Å Ar$^+$ laser radiation. The intensity of the Q branch of the anti-Stokes scattering $(v=1 \rightarrow v=0)$ at 4382 Å was measured because the anti-Stokes spectra are free of Raman scattering from the $N_2(v=0)$ level (whereas the Stokes transitions from $v=1 \rightarrow v=2$ lie in the rotational structure of the Stokes lines from $v=0 \rightarrow v=1)$.

The experimental arrangement is shown schematically in Fig. 1. Molecular nitrogen is partially dissociated by a microwave discharge in a flow system having a linear velocity of 400 cm sec^{-1}. The nitrogen atoms can be titrated with NO at any of six fixed inlet jets at 8, 15, 30, 42, 65, and 100 cm from the pyrex cell (referred to as inlets 1 through 6, respectively). The output of an Ar$^+$ ion laser (Coherent Radiation Model 52B) traverses the cell and is focused to a point within it. This focal point is imaged on the slit of a spectrometer (Spex Model 1402) by a second optical system. The light passing through the exit slit of this spectrometer is imaged on the photocathode of a 6256S photomultiplier. Its output is measured in a pulse-counting system and then printed out after a predetermined counting time (governed by the setting of the controller).

Initial experiments were made to determine the magnitude of the interference from emissions of the titrated afterglow. The nature of this problem can be seen in Fig. 2, which shows the light signal at 4382 Å from the afterglow as a function of NO addition. The signal reaches a minimum of ~ 10 counts sec^{-1} (which includes a dark count of ~ 5 sec^{-1}) when the NO is just sufficient to remove the N atoms by reaction (2) (called "null"). Further addition of NO generates the NO_2 continuum by the reaction of the excess NO with the oxygen atoms, that is,

$$NO + O + M \rightarrow NO_2^* + M \quad , \tag{4}$$

A-4

followed by

$$NO_2^* \rightarrow NO_2 + h\nu \quad (3875\text{-}14{,}000 \text{ Å}) \quad . \tag{5}$$
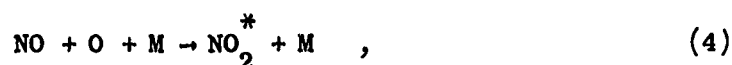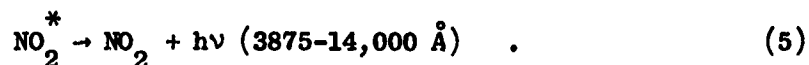
Thus when NO is in excess, radiation from (5) is transmitted by the spectrometer at 4382 Å.

When insufficient NO is added, the signal arises from the generation of NO β bands by the chemiluminescent recombination of oxygen and nitrogen atoms, that is,

$$N + O + M \rightarrow NO \; (B^2\Pi_r) + M \tag{6}$$

$$NO(B^2\Pi_r) \rightarrow NO \; (X^2\Pi_r) + h\nu(\beta \text{ bands}) \quad . \tag{7}$$
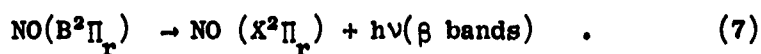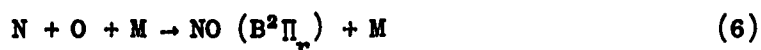
The light being transmitted by the spectrometer at 4382 Å is in the tail of the (0,13) band, whose head is at 4309.7 Å (the bands are degraded to longer wavelengths). (The bandpass of the spectrometer ($\sim$ 1·1 Å) was such as not to transmit any of the short wavelength head of the (1,14) band at 4385·7 Å.)

The trace on Fig. 2 clearly demonstrates the need to maintain the NO addition as close to the null point as possible. To do this the valve controlling the NO addition was coupled to a servo-controlled motor. The inputs to the motor controller were derived from two 1P21 photomultipliers viewing the afterglow downstream of the pyrex cell. One photomultiplier "sensed" the continuum through a 5622 Å interference filter (10 Å half-width), while the other viewed the afterglow through a Kodak 18A filter and was therefore sensitive only to the NO β bands. With this arrangement, it was possible to maintain the NO addition within 1% of null. Therefore, for Raman measurements on the titrated afterglow, the servo-controlled motor was always used to regulate the NO addition.

A-5

Since reaction (2) is the well-know titration reaction for nitrogen atoms the partial pressure of nitrogen atoms being reacted with NO was determined in the following manner. With the microwave discharge on the servo-controlled motor was used to regulate the NO addition to the null position at which the partial pressure of NO being added equals the partial pressure of nitrogen atoms in the afterglow. The NO partial pressure being added was then determined by turning both the servo-controlled motor and the microwave discharge off and determining the change in the system pressure when the NO was turned off, using a differential pressure diaphragm transducer attached to the vacuum system downstream of the Pyrex cell. This pressure change was too small for accurate measurement with 100% NO so an analyzed mixture of 10% NO in helium was used for the measurements.

The measurements were made with an EMI 6256S phototube with 20-dB attenuation inserted in the line between the photomultiplier base and the photon counter, to provide the greatest freedom from rf pickup. The best signal-to-dark count was obtained with 1200 V on the photomultiplier, which resulted in a counting efficiency 75% of the plateau maximum and a dark count of ~ 5 sec^{-1}.

Before making any Raman measurements, the positions of lenses L_1 and L_2 were adjusted to provide the biggest Rayleigh-scattered light signal (with N_2 at 600 torr in the cell) using the 4579 Å laser line (the shortest wavelength laser line and hence that closest in wavelength to the position of the anti-Stokes line at 4382 Å). This focus was periodically checked but was found to require minimum adjustment. The wavelength error in the readout of the spectrometer was periodically checked with the 4358.3 Å line of Hg. It did not change during the course of these measurements.

In addition to several photomultiplier counts per second originating from the titrated afterglow, a small signal (< 0.03 counts/sec) at 4382 Å was also produced by the laser (arising from the 4379.7 Å argon line emitted by the discharge in the laser cavity). Because of these two sources of background, the Raman signal had to be extracted from the counts C_1 obtained in four consecutive counting periods of equal length. From such a sequence, which we define as an "experiment," the Raman signal is obtained from

$$\text{Raman counts} = C_2 + C_4 - C_1 - C_3 \quad , \tag{8}$$

where C_2 is the count obtained with the microwave discharge and laser on (and hence includes the Raman signal together with the scattered light from both sources and the dark count); C_4 is the photomultiplier dark count (microwave discharge and laser off); C_1 is the count with only the microwave discharge on; and C_3 is the count with only the laser on. For most of the experiments, the counting period was six minutes.

It was soon discovered that, even without titrating the N atoms, the $N_2(v=1)$ present in the afterglow was sufficient to produce a large Raman signal (increasing from 0.5 to 20 counts/sec as the N_2 pressure was raised from 1.5 to 12 torr). To increase the detectability of the $N_2(v=1)$ expected from the N + NO reaction, it was decided to remove or at least minimize the $N_2(v=1)$ originating in the discharge. This was done by inserting a glass-wool plug between the discharge and the NO-inlet positions. The logic behind this approach, which has been used before[11-13] is that the deactivation of $N_2(v=1)$ on pyrex surfaces ($\gamma = 4.5 \times 10^{-4}$) is more efficient than the removal of nitrogen atoms ($\gamma = 2 \times 10^{-5}$).[17-19] The first two trials of a glass-wool plug confirmed this situation, reducing the $N_2(v=1)$ in N_2 at 6 torr by factors of 3 and 5, while reducing the nitrogen atoms by 10 and 25%, respectively. Several large glass-wool

plugs were tried--the largest decreasing the $N_2(v=1)$ in N_2 at 6 torr by a factor of 30 (to ~ 0.3 counts/sec) while reducing the nitrogen atoms by two (to ~ 8 mtorr). Most of the measurements to be described were made under these conditions. The final measurements were made with a 5% N_2 in argon mixture at 10 torr (with the largest pyrex wool plug in place), which reduced the $N_2(v=1)$ signal with no titration by another factor of five (to ~ 0.06 counts/sec) while only reducing the N atoms by another 40% (to ~ 5 mtorr).

Because it took many minutes for the microwave discharge to stabilize, it was found preferable to leave the microwave discharge on all the time and to evaluate the Raman counts plus a small signal due to the laser scattered light from:

$$\text{Raman counts + laser scattered light} = C_2 - C_1 = S \ . \qquad (9)$$

This was determined for both the untitrated afterglow ($= S_{untitrated}$) and the titrated afterglow when the titration was performed at inlets no. 1, 2, 3, 4, and sometimes 5. The titrated signals were then plotted as a function of distance from the titration point to the cell and extrapolated to zero distance to determine the signal S_o, that would have been produced if there had been no loss of $N_2(v=1)$ between the titration point and the cell. From this signal, $S_{untitrated}$ was subtracted to obtain the signal produced by reaction (2), ($S_{reaction}$). The subtraction removes the small signal from the scattered laser light which is present in both S_o and $S_{untitrated}$.

III. CALIBRATION

To convert the net measured Raman signal into a partial pressure of N_2(v=1) at 297°K, we measured the intensity of the anti-Stokes line at 4382 Å with nitrogen at atmospheric pressure in the cell. Table I shows the data obtained using a chromel-alumel thermocouple to measure the nitrogen temperature. The last column corrects the actual pressure of N_2(v=1) to the equivalent pressure at 297°K. This is shown plotted against photomultiplier counting rate in Fig. 3. The horizontal error bars show the effect of an uncertainty of ± 2°K in the gas temperature. The straight line drawn gives a sensitivity of 41 counts/sec [torr N_2(v=1)]$^{-1}$. This experiment was repeated several times during the measurement program and was always found to lie within a range 41 ± 3 counts/sec [torr N_2(v=1)]$^{-1}$.

Because thermal conduction might affect the thermocouple readings, we also determined the gas temperature from the intensity variation of the rotational Raman spectrum. This rotational Raman spectrum is of high quality, and provides a reliable temperature measurement. The intensity formula is[20]

$$I = f(\nu)\ \nu^3 S_J \exp(-BJ(J+1)hc/kT) \quad , \tag{10}$$

where $f(\nu)$ incorporates the possible frequency dependence of the counting efficiency, S_J is the line strength, and the ν^3 variation must not be ignored if the correct T is to be obtained. The Stokes lines progress to larger wavelengths with J, and the anti-Stokes lines progress to smaller wavelengths, but they give a common temperature to within ± 1°K

29

when $f(\nu)$ is assumed constant. This indicates that the frequency dependence of the counting efficiency is negligible over the range (~ 100 Å) of the rotational spectrum. The resulting rotational temperature agrees with the thermocouple reading at room temperature, and the thermocouple reading was about $4°K$ low when the rotational temperature was $377°K$. We have therefore made a linear correction to the thermocouple reading, varying from 0% at $297°K$ to + 1% at $373°K$. These corrected temperatures are used in Table I.

TABLE I. Photomultiplier Count Rate and Pressure
of $N_2(v=1)$ in N_2 at Various Temperatures

Temperature $(T°K)$	Photomultiplier Signal (counts/sec)	$\dfrac{[N_2(v=1)]}{[N_2(v=0)]}$	$[N_2(v=1)]$ (Torr in N_2 at 760 Torr)	$[N_2(v=1)] \times \dfrac{297}{T\ K}$ Torr
297	5.44	1.25×10^{-5}	0.0095	0.0095
323	5.89	3.10×10^{-5}	0.024	0.022
350	6.88	6.90×10^{-5}	0.053	0.045
364	7.49	9.98×10^{-5}	0.076	0.062
379	8.51	1.44×10^{-4}	0.109	0.086

IV. RESULTS

The Raman counts obtained from the titration were about 1 sec^{-1}, and this signal had to be measured in the presence of a dark count of 5 sec^{-1} and several counts per second produced by light from the titrated afterglow. Therefore a large number of experiments had to be performed at each titration point to determine the signal with sufficient accuracy. Table II is an example of the data obtained in approximately six hours at one titration point. This data point and the ones determined when titrating at inlets no. 1, 3, 4 and 5 are shown in Fig. 4. It can be seen that, with increasing distance, the signals obtained for the titrated afterglow appear to be asymptotic to the value obtained for the untitrated afterglow. This is because the microwave discharge produces so much more $N_2(v=1)$ than the titration that as the titration point moves further from the Pyrex cell and closer to the discharge, the $N_2(v=1)$ produced by the titration reaction becomes a smaller and smaller fraction of the $N_2(v=1)$ surviving from the discharge. The error bars are the estimated error of the mean, $p_{\bar{x}}$, determined from

$$p_{\bar{x}} = \frac{\sigma_x}{\sqrt{N}} \tag{11}$$

where σ_x is the standard deviation of the individual x values and N is the number os such values. At various times during the measurement the NO was turned off and the Raman signal from the untitrated afterglow was determined, to ensure that neither the optical focus nor the afterglow condition had changed.

The result obtained in four separate series of measurements are shown in Table III. They have been arranged in order of decreasing Raman signals from the untitrated afterglow. The Raman signal produced by the

TABLE II. Signal Obtained by Titrating 8 mtorr

of N Atoms at Inlet No. 2

$$(N_2 = 6 \text{ torr})$$

Expt. No.	Laser off C_1 Counts	Laser on C_2 Counts	$C_2 - C_1$ Counts	Expt. No.	Laser off C_1 Counts	Laser on C_2 Counts	$C_2 - C_1$ Counts
1	3884	4196	312	15	3958	4189	231
2	3875	4329	454	16	4060	4235	175
3	4028	4197	169	17	3939	4250	311
4	3694	4204	510	18	3890	4384	494
5	3949	4116	167	19	3959	4213	254
6	3948	4106	153	20	4053	4248	195
7	3848	4044	196	21	4003	4219	216
8	3921	4095	174	22	3903	4381	478
9	3970	4393	423	23	4029	4370	341
10	3851	4191	340	24	4063	4321	258
11	4000	4202	202	25	3949	4262	313
12	3965	4333	368	26	3998	4304	306
13	3784	4215	431	27	4047	4349	302
14	3932	4289	357	28	4012	4526	514

Note: Counts in a 6 minute period. Signal
from untitrated afterglow = 107 ± 11

Mean $\bar{x}$ = 309

Number of measurements, N = 28

σ_x = 115

Estimated error of mean $p_{\bar{x}} = \dfrac{\sigma_x}{\sqrt{N}} = 22$

TABLE III.   Efficiency with which the Exothermicity of the
Reaction of Nitrogen Atoms with Nitric Oxide is
Converted into Vibrational Energy.

Gas	Pressure	$S_{untitrated}$ (counts/sec)	S_o (counts/sec)	$S_o - S_{untitrated}$ $= S_{reaction}$ (counts/sec)	$N_2(v=1)$ (mtorr)	N (mtorr)	F
N_2	6 Torr	1.17	2.18	1.01	25	11	0.20
N_2	6 Torr	0.30	1.11	0.81	20	8.0	0.22
N_2	6 Torr	0.29	1.12	0.83	20	7.5	0.24
5% N_2/ argon	10 Torr	0.056	0.68	0.62	15	5.5	0.25

reaction is shown in column 5 and is then converted to a $N_2(v=1)$ pressure
using the sensitivity of 41 counts/sec $[torr\ N_2(v=1)]^{-1}$ -- this is shown
in column 6.   Column 7 shows the N atom pressure.   The efficiency with
which the exothermicity of the reaction is converted into vibrational
energy is shown in the final column.   This efficiency, F, is calculated
from

$$F = \frac{P_{N_2(v=1)}}{11.3\ P_N}$$ (12)

A-13

where $P_{N_2(v=1)}$ is the partial pressure of $N_2(v=1)$ produced by reacting a partial pressure, P_N, of nitrogen atoms with NO and the factor 11.3 is introduced because the exothermicity of the reaction (3.27 eV) is 11.3 times the vibrational energy of $N_2(v=1)$ [0.289 eV].

The value of F determined with 5% N_2 in argon at 10 torr has been increased by 6% above that calculated from Eq. (12) to allow for the Boltzmann population in the v=2 level (for a vibrational temperature of $960°K$). This is a negligible correction in the other three sets of experiments with N_2 at 6 torr, because in these cases the N_2 vibrational temperature was much smaller ($\leq 610°K$).

V. DISCUSSION

The value of F in Table III tends to increase as the background ($S_{untitrated}$) is reduced. It was originally thought that this might reflect an increased rate of decay of $N_2(v=1)$ in the presence of oxygen atoms (produced by reaction (2)) compared to when only nitrogen atoms are present. Part of this increased rate of decay might involve the V-T relaxation of $N_2(v=1)$ by $O(^3P)$, which has recently[21] been shown to have a rate of 3.5×10^{-15} cm^3 $molec^{-1}$ sec^{-1} and part might arise from an increased catalytic efficiency of the walls. However, extrapolating the measurements to zero distance should remove any homogeneous or wall decay between the inlet jet and the cell. The possibility remains that the walls of the inlet jet itself or hot $O(^3P)$ produced in the vicinity of the inlet jet by reaction (2) could deactivate $N_2(v=1)$. These effects would not be allowed for by the extrapolation to zero distance. It is for these reasons that the values obtained with the lowest background from the discharge are to be most trusted. With this in mind and allowing for possible errors in the extrapolation to determine S_o and in measuring the N atom concentration and the sensitivity to $N_2(v=1)$, we

A-14

recommend a value of 0.25 ± 0.03 for the efficiency with which the exothermicity of reaction (2) appear as N_2 vibrational energy.

It should also be noted that the last value of F in Table III was obtained with only 0.5 torr of N_2 (+ 9.5 torr of argon) and is in agreement with the measurements at N_2 = 6 torr. This requires that 0.5 torr of N_2 be more than sufficient to Boltzmannize the initial distribution of vibrational levels in a flow time of 0.02 sec (8 cm at 400 cm sec^{-1}). This corresponds to a rate coefficient $> 3 \times 10^{-15}$ cm^3 $molec^{-1}$ sec^{-1} which is much faster than the value of 3.5×10^{-16} cm^3 $molec^{-1}$ sec^{-1} found by Phillips and Schiff[12] for collisional deactivation of $N_2(v)$ to vibrational levels below the fourth. The reason for this discrepancy is not apparent although Wray[14] has questioned the low rate found in the earlier work. [A possible explanation, which seems very unlikely but cannot be excluded, is that decomposition of ozone is possible by stepwise excitation of ozone by levels below v = 4.]

The measurement with 5% N_2 in argon shows that the vibrationally excited nitrogen is a product of the reaction (2) and is not subsequently excited by collisions of translationally hot oxygen atoms, produced by reaction (2), with N_2. If this latter process were involved the large excess of argon over nitrogen in the latter measurement would thermalize the hot oxygen atoms and prevent vibrational excitation of N_2. Hence Wray's criticism of the earlier work[11-13] on this reaction does not appear to be valid. In fact the value obtained by Schiff and his coworkers (F = 0.27 ± 0.06) is in agreement with our value despite the nonspecific nature of their calorimetric detector.

ACKNOWLEDGEMENTS

[1] L. Thomas and R. B. Norton, J. Geophys. Res. 71, 227 (1966).

[2] A. L. Schmeltekopf et al., Planet. Space Sci. 15, 1097 (1967).

[3] A. L. Schmeltekopf, E. E. Ferguson, and F. C. Fehsenfeld, J. Chem. Phys. 48, 2966 (1968).

[4] A. Dalgarno, M. B. McElroy, and J. C. G. Walker, Planet. Space Sci. 15, 331 (1967).

[5] J. C. G. Walker, Planet. Space Sci. 16, 321 (1968).

[6] J. C. G. Walker, R. S. Stolarski, and A. F. Nagy, Ann. Geophys. 25, 831 (1969).

[7] E. Bauer, R. Kummler, and M. H. Bortner, App. Optics 10, 1861 (1971).

[8] E. Fisher and E. Bauer, J. Chem. Phys. 57, 1966 (1972).

[9] G. Black and D. J. Eckstrom, "Excitation and Deexcitation of Vibration in N_2 by Oxygen Atoms," Final Report, SRI Project 8626, October 1971.

[10] The value of $8.3 \pm 6.5\%$ quoted in Ref. 9 is inversely related to the lifetime of $N_2(v=1)$ in the pyrex reaction cell, for which a value of 1 sec was assumed. The present measurements of the decay of $N_2(v=1)$ with distance from the pyrex cell show a $1/e$ decay in ~ 40 cm distance, which corresponds to a lifetime of ~ 0.1 sec. Because the diffusion time is proportional to radius and the pyrex cell has approximately twice the

radius of the inlet tubing (also pyrex), the lifetime in the cell is

~ 0.2 sec. This changes our value to $42 \pm 33\%$, which neither supports

nor refutes the theoretical calculation. Clearly, further experimental

work on this reaction is desirable.

[11] J. E. Morgan, L. F. Phillips, and H. I. Schiff, Disc. Faraday

Soc. 33, 118 (1962).

[12] L. F. Phillips and H. I. Schiff, J. Chem. Phys. 36, 3283 (1962).

[13] J. E. Morgan and H. I. Schiff, Can. J. Chem. 41, 903 (1963).

[14] K. L. Wray, E. Feldman, and P. Lewis, J. Chem. Phys. 53, 4131

(1970).

[15] W. D. Breshears and P. F. Bird, J. Chem. Phys. 48, 4768 (1968).

[16] D. L. Baulch et al., "Critical Evaluation of Rate Data for

Homogeneous, Gas Phase Reactions of Interest in High-Temperature Sys-

tems," School of Chemistry, The University, Leeds, England, No. 4

(December 1969).

[17] J. T. Herron et al., J. Chem. Phys. 30, 879 (1959).

[18] T. Wentinck, Jr., J. O. Sullivan, and K. L. Wray, J. Chem. Phys.
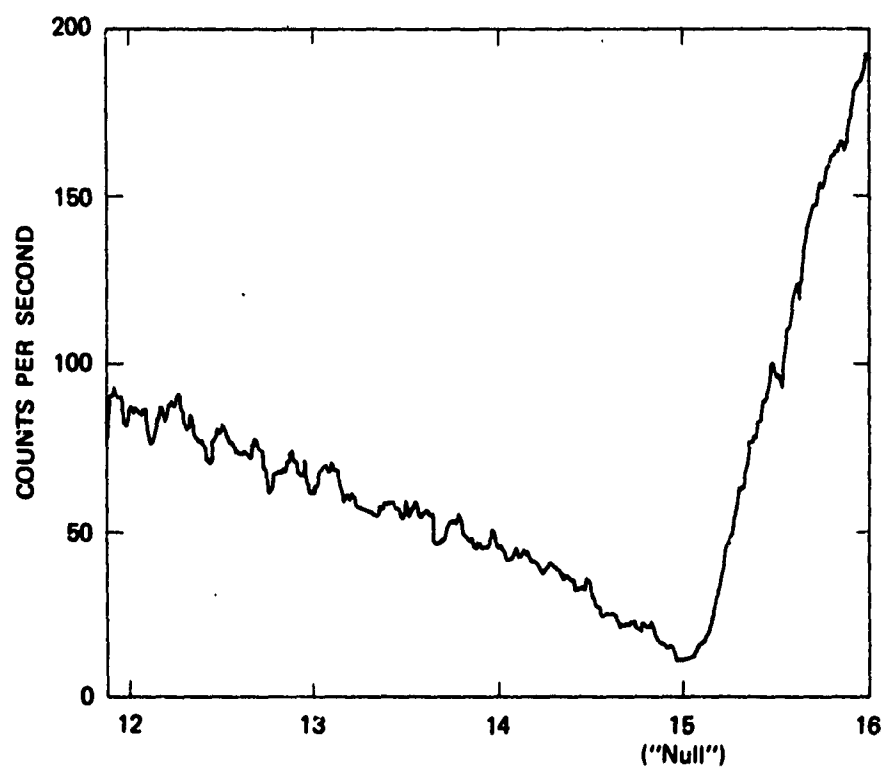
29, 231 (1958).

[19] R. A. Young, J. Chem. Phys. 34, 1292 (1961).

[20] G. Herzberg, "Molecular Spectra and Molecular Structure. I.

Spectra of Diatomic Molecules," p. 127, D. Van Nostrand Company, Inc.,

1950.

[21] P. J. McNeal, M. E. Whitson, and G. R. Cook, Chem. Phys. Letters,
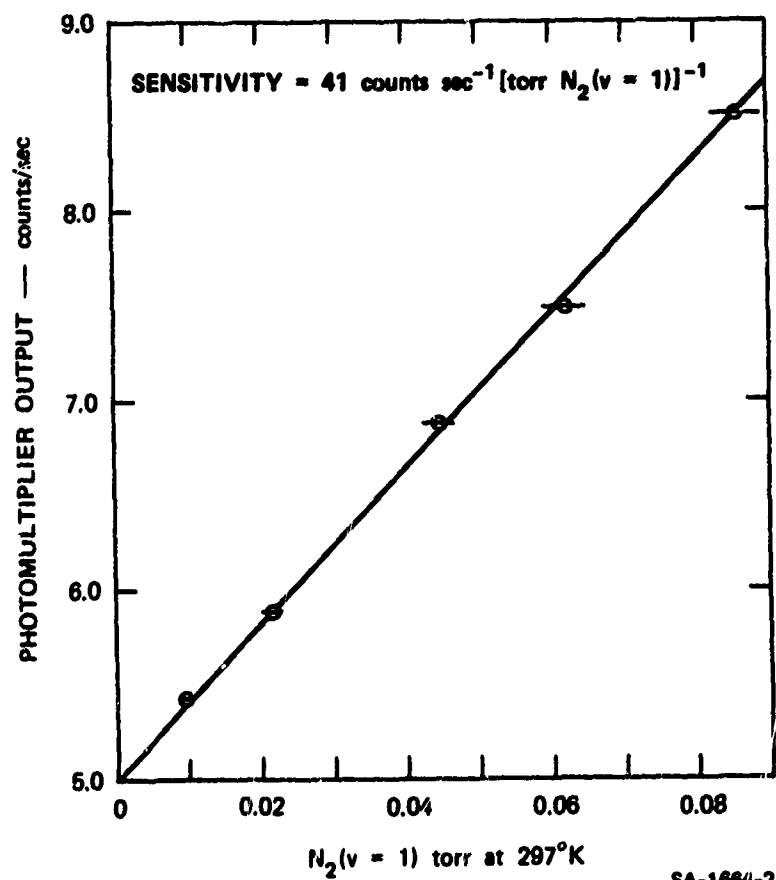
16, 507 (1972).

FIGURE CAPTIONS

Fig. 1   Experimental arrangement for Raman spectroscopy. The lens
L_2, which has an aperture ratio of $f/0.95$ and a focal length
of 5 cm, collects the Raman-scattered light over a large
solid angle. The titrated afterglow enters the pyrex cell
immediately above the focus of the laser beam.

Fig. 2   Light signal at 4382 Å from microwave-discharged N_2 at
3 torr as a function of NO addition close to the equiv-
alence point ("null"). Spectrometer bandpass $\sim 1 \cdot 1$ Å.
Titration performed 100 cm ($\sim 0 \cdot 25$ second flow time)
from cell.

Fig. 3   Determination of the experimental sensitivity to $N_2(v=1)$
using heated N_2.

Fig. 4   Raman signal produced when 8 mtorr of nitrogen atoms are
reacted with NO at various distances from the center of
the pyrex cell. N_2 = 6 torr. With no titration a Raman
signal of $0 \cdot 30$ counts/sec is present in the afterglow.

TA-8626-IR4

NO ADDITION — x 10^{-3} torr

SA-1664-1

35

SENSITIVITY = 41 counts sec^{-1} [torr N$_2$(v = 1)]$^{-1}$

PHOTOMULTIPLIER OUTPUT — counts/sec

N$_2$(v = 1) torr at 297°K

SA-1664-2

36

$S_O = 1.11$ counts sec^{-1}

$S_{untitrated} = 0.30$ counts sec^{-1}

RAMAN SIGNAL — counts/sec

DISTANCE FROM TITRATION POINT TO CENTER OF PYREX CELL
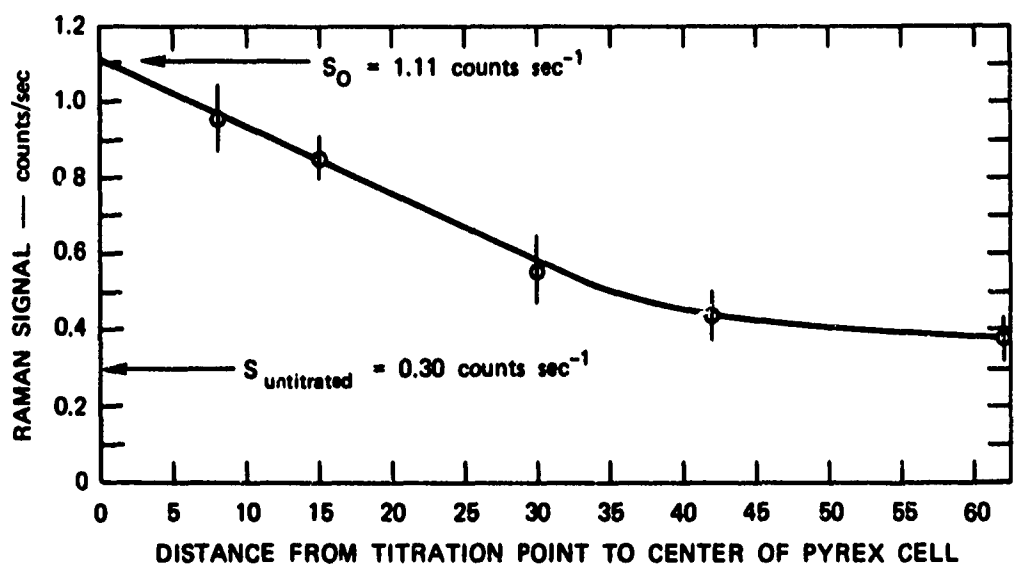
SA-1664-3

APPENDIX B

VIBRATIONAL RELAXATION OF SHOCK-HEATED N_2 BY ATOMIC
OXYGEN USING THE IR TRACER METHOD

D. J. Eckstrom

APPENDIX B

VIBRATIONAL RELAXATION OF SHOCK-HEATED N_2 BY ATOMIC OXYGEN USING THE IR TRACER METHOD

D. J. Eckstrom

Molecular Physics Department, Stanford Research Institute
Menlo Park, California - 94025

ABSTRACT

We have studied the effects of oxygen atoms on the vibrational relaxation of shock-heated N_2 over the temperature range from 1200 to 3000 K, using the CO tracer technique. The measured relaxation times $p\tau_{N_2-O}$ vary from 0.8 to 2 atm-μs in this range with an uncertainty of $\pm$ 50%, which is in excellent agreement with existing high-temperature shock tube and low-temperature flow tube results. The weak temperature dependence of all of these results is in marked contrast to theoretical predictions. However, the relatively fast relaxation rates at low temperatures verified by these measurements allow a satisfactory explanation of the observed vibrational temperature of N_2 in the upper atmosphere.

Some limited measurements of the relaxation of CO by oxygen atoms yield values of $p\tau_{CO-O}$ of approximately 0.04 atm-μs. This is approximately the same as $p\tau_{O_2-O}$, and probably is indicative of the importance of atom-exchange processes in both of these reactions.

I INTRODUCTION

A number of experiments have been reported in which the vibrational relaxation of a diatomic gas by a chemically active atomic species was studied. These include shock tube studies of the effects of $O(^3P)$ on O_2 by Kiefer and Lutz,[1] of $O(^3P)$ on N_2 by Breshears and Bird,[2] of H on CO and of Fe on CO by von Rosenberg, et al.[3,4] Very recently, McNeal, Whitson, and Cook[5] have reported low-temperature measurements in a flowing afterglow of the effect of $O(^3P)$ on N_2. In all cases, the relaxation times for these diatom-atom collisions are considerably shorter than would be predicted from correlations based on reduced mass (e.g., Millikan and White[6]); furthermore, the relaxation times generally show very little temperature-dependence.

For the $O-O_2$ and $O-N_2$ cases, and speculatively for the Fe-CO case, the rapid vibrational energy transfer has been attributed to a "chemical" effect since in each case there can be an attractive chemical bond. Fisher and Bauer,[7] using a curve-crossing model, have made calculations for the $O-N_2$ system that predict the high-temperature results of Breshears and Bird. Their assumed potential for the interaction of N_2 with O gives an activation energy of 0.8 eV; as a result, their calculated results show a very strong temperature-dependence. Therefore, their predicted room temperature relaxation rate is more than 8 orders of magnitude slower than the experimental results of McNeal, et al.

Breshears and Bird's measurements with the laser schlieren technique covered the temperature range from 3000 to 4500 K. The lower temperature limit was imposed by the onset of large random fluctuations in the schlieren signal that were probably caused by turbulence in the shock tube boundary layers. We report here the results of a program undertaken

to extend the lower temperature limit of the shock tube measurements of the $O-N_2$ system to approximately 1000 K by the use of the CO infrared tracer technique.[8] This method has been used to measure the relaxation of N_2 and of N_2-O_2 mixtures for temperatures as low as 800 K,[8-10] which is well below the limit for interferometry or laser schlieren measurements for these gases. The CO tracer method has a shortcoming, however, in that it introduces additional species into the gas mixture, namely CO and CO_2, whose effects on the N_2-O system must be considered. Also, as described later, components of IR radiation in addition to the desired CO signal can possibly interfere with the measurements.

As in the other shock tube studies of the effects of O atoms, the ground state $O(^3P)$ atoms are obtained from the shock-heated thermal dissociation of O_3 added to the test gas mixture. The primary reactions of interest are

$$O_3 + M \rightarrow O + O_2 + M \quad , \tag{1}$$

$$O + O_3 \rightarrow O_2 + O_2 \tag{2}$$

and

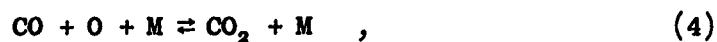$$O_2 + M \rightleftharpoons O + O + M \quad , \tag{3}$$

where M is any collision partner, predominantly N_2. At high temperatures, the dissociation of O_3 is dominated by reaction (1), and there is virtually a one-to-one conversion of O_3 to O atoms. At lower temperatures, however, reaction (2) becomes increasingly important so that relatively fewer O atoms are produced. The rates for these processes, their uncertainties, and the fractional production of O atoms are discussed in the Appendix.

The decomposition of O_3 behind the shock wave by reactions (1) and (2) is accomplished in less than 1 us for the conditions of these tests, while reaction (3) is much slower than vibrational relaxation processes

B-3

and is therefore unimportant. Three other reactions of possible importance are:

$$CO + O + M \rightleftharpoons CO_2 + M \quad , \qquad\qquad (4)$$

$$CO + O_2 \quad \rightleftharpoons CO_2 + O \quad , \qquad\qquad (5)$$

and

$$O + N_2 \quad \rightleftharpoons NO + N \quad . \qquad\qquad (6)$$

Again, an examination of the rates for these processes indicates that they are slow compared with vibrational relaxation processes. Therefore, we can assume that the concentration of O atoms is constant during the time interval of interest.

II EXPERIMENTAL

The shock tube used in this study is a stainless steel tube 5 cm
in diameter by 4 m long, operated with cold H_2 pressure drive. The
test station 40 cm from the endwall was fitted with a sapphire infrared
window and with two quartz windows for UV absorption measurements. An
InSb photovoltaic detector was focussed on the center of the shock tube
using an IRTRAN II lens. The infrared optical alignment was accomplished
by maximizing the chopped radiation signal from a small thermal source
placed at the shock tube axis. A narrow-bandpass filter (5.05 to 5.15 μ)
was used in all tests. In most of the experiments, the detector was
used in the voltage mode, and the signal amplified by an operational am-
plifier having a gain of 50. The response time of this detector-amplifier
configuration was determined to be 1.6 μs when an IR LED and an HP 8002A
pulse generator with 10 ns risetime were used. Late in the program, an
automatically biasing current mode amplifier was obtained. The response
time was then reduced to less than 1 μs. For all the data discussed
here, the intensity risetime was several times the detector response
time.

The N_2-CO and N_2-CO-O_2 gases used in the study were premixed by
Matheson and were of at least 99.995% purity. Ozone was made by dis-
charging O_2 and condensing the resulting O_3 at liquid N_2 temperatures.
The N_2-CO-O_3 mixtures were then made by using the premixed N_2-CO after
passage through a Millikan-type cold trap,[11] with pressures measured on
calibrated Wallace and Tiernan gages. These test samples were stored
at dry ice temperatures to reduce decomposition of the O_3; samples were
generally made daily. The actual concentration of O_3 in each test gas
fill was measured by 2537 Å UV absorption at the shock tube test station,
assuming an absorption coefficient of 300/cm-atm. From the difference

B-5

between the concentration at mixing and at testing, the decomposition could be deduced. These measurements gave the mole fraction of O_3 accurate to approximately 0.05%, and showed decomposition increasing with time from 0 to 30% of the initial O_3 concentration. A separate study of the decomposition process by IR absorption showed that at dry ice temperature a maximum of 30% of the O_3 lost was converted to CO_2, and this amount of CO_2 can be assumed to have been present as an impurity in the test gas samples.

Before each shock tube test, the tube was evacuated and then filled with a passivation sample of pure O_3. After approximately 10 minutes, the tube was again evacuated to 10^{-5} torr, at which point the combined leak and outgassing rate was about 2×10^{-4} torr/minute. The tube was sealed, filled with test gas, and the shot fired within 3 minutes. As noted above, the actual O_3 concentration in the test gas sample was measured by UV absorption, and total sample pressure was measured both by calibrated Wallace and Tiernan gages and by a sulfuric acid manometer. Total pressures varied from 2 to 150 torr and were measured to an uncertainty of less than 5%. The shock velocity was measured with thin film heat transfer gages with an uncertainty of less than 2%. The combined uncertainties of the physical quantities (pressure, temperature, relaxation time, and the like) were approximately ± 20%.

44

III OBSERVATIONS

To establish baselines for the effects of O atoms on the vibrational relaxation of N_2, a series of preliminary tests were made on N_2-1% CO, N_2-5% CO, and N_2-1%CO-5% O_2 mixtures. Results from these experiments are presented in Figure 1, together with curves representing earlier results for similar mixtures obtained by Millikan and White.[8,9] The "pure" N_2 results can be seen to agree very well over their common temperature range, although there is a deviation from a straight-line extrapolation at temperatures below about 2000 K. Such a deviation could be caused by small concentrations of impurity gases, and, in part, by the CO gas. The latter effect is demonstrated by the different results for mixtures containing 1 and 5% CO. The results for the N_2-O_2 mixture also show good agreement with the earlier results.[9] The N_2-O_2 measurements of this study were limited to temperatures below 2600 K by extraneous radiation that obliterated the relaxation profile. To study this problem, some experiments also were conducted with radiation filters that passed shorter wavelengths; in these tests, the extraneous radiation occurred at even lower temperatures, leading to speculation that the radiation is from CO_2 formed by reaction between CO and O_2. Another possibility is that the radiation arises from H_2O formed by combustion at the contact surface, and the radiation diffuses forward through the CO.

In the N_2-CO and N_2-CO-O_2 tests, the CO radiation showed a single exponential risetime characteristic of an IR tracer method in which the vibrational temperature of the tracer gas is completely equilibrated with that of the N_2. When O_3 is added to the test gas mixture, however, the radiation exhibits a double exponential behavior as shown in a typical oscilloscope trace and a semilogarithmic plot of that trace in Figure 2.

B-7
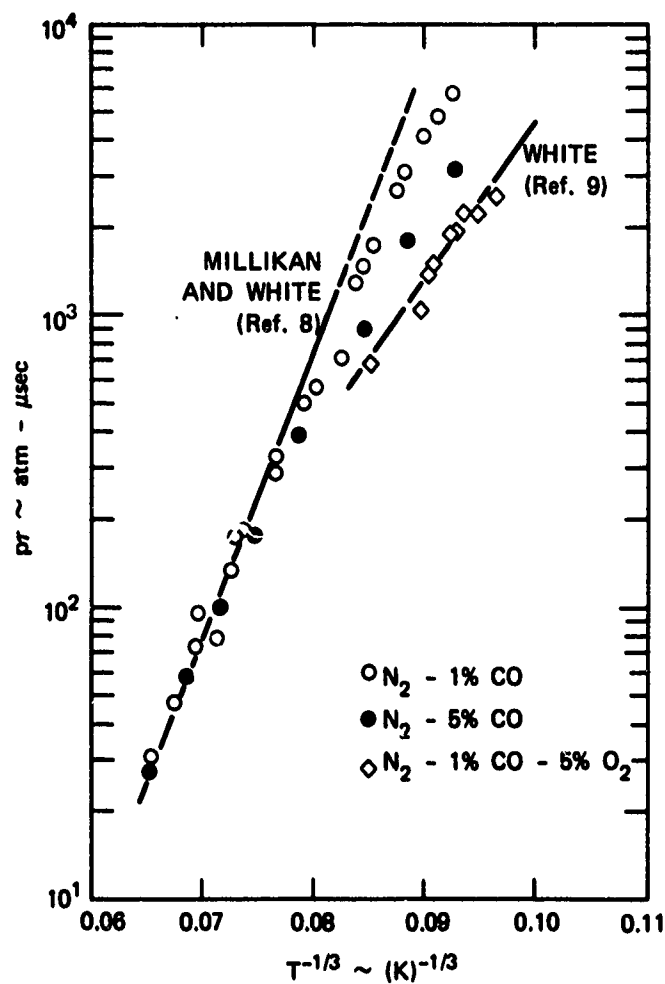
SA-1664-6

FIGURE 1   VIBRATIONAL RELAXATION TIMES FOR
N_2 - CO AND N_2 - CO - O_2 MIXTURES
BY THE IR TRACER METHOD
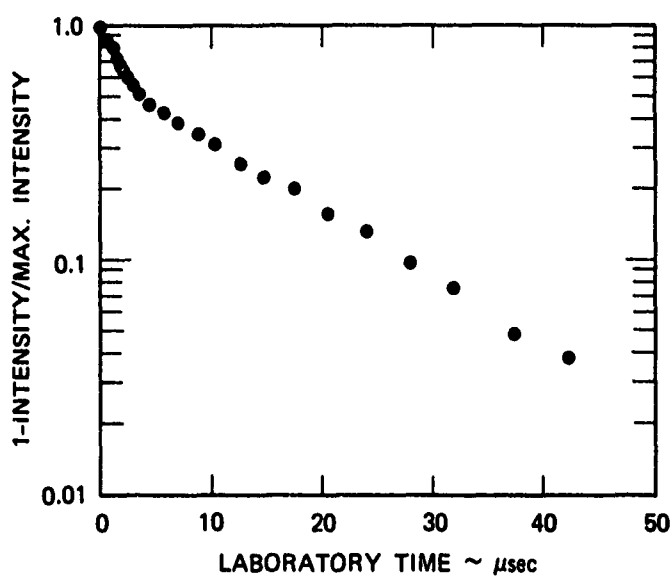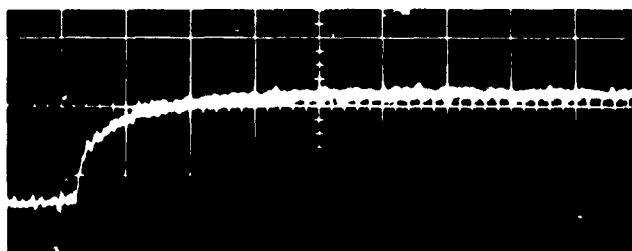
FIGURE 2   TYPICAL INTENSITY HISTORY
(MACH 4.8, p_1 = 45 torr, T_2 = 1530 K)

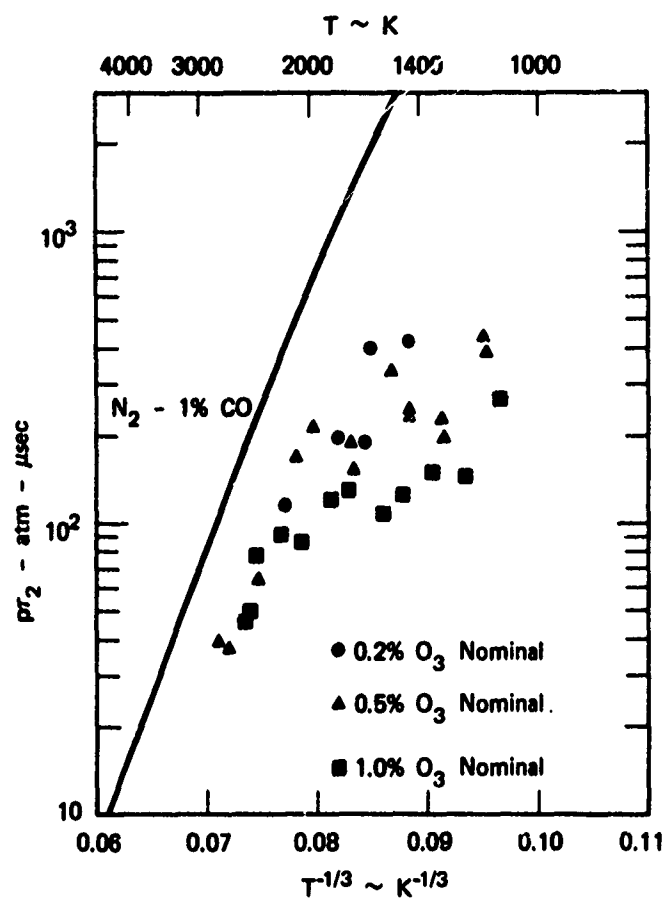SA-1664-10

B-9

47

This type of behavior, as observed and discussed previously by Taylor, Camac, and Feinberg,[12] and by Sato, Tsuchiya and Kuratani[13] normally indicates that the CO has relaxed independently to a considerable extent before it couples to the N_2. The initial risetime τ_1 then gives the rate of relaxation of CO in the mixture. As discussed in a following section, however, this does not seem to be the complete explanation in these tests. The second time constant τ_2 in all cases is related to the N_2 relaxation rate. A very limited number of tests were conducted with an Ar-1% CO-1%O_3 mixture. In these tests, the radiation again showed a single exponential risetime of CO relaxation governed by the effects of O atoms.

A series of tests was conducted at each of the nominal O_3 concentrations of 0.2, 0.5, and 1.0%. The experimental mixture relaxation times, $p\tau_2$, for these nominal concentrations are presented in Figure 3. As observed also by Breshears and Bird,[2] even these very small concentrations of O_3 (and consequently O atoms) produce substantial reductions in the observed N_2 relaxation times (e.g., nearly two orders of magnitude for 1% O_3 at 1000 K). Because it was not always possible to add exactly the desired amount of O_3 to the test gas mixtures, and because of decomposition, the actual O_3 concentrations deviated from the nominal values by up to 50%. This contributes to the scatter of the data in Figure 3.
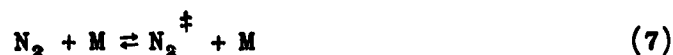
FIGURE 3   VIBRATIONAL RELAXATION TIMES FOR
N₂ IN A MIXTURE CONTAINING OXYGEN
ATOMS

SA-1664-11

B-11

IV ANALYSIS

Because of the many species present, the number of vibration-translation (V-T) and vibration-vibration (V-V) processes taking place in the gas mixture is large. We can summarize the possible V-T processes as

$$N_2 + M \rightleftharpoons N_2^{\ddagger} + M \tag{7}$$

$$O_2 + M \rightleftharpoons O_2^{\ddagger} + M \tag{8}$$

$$CO + M \rightleftharpoons CO^{\ddagger} + M \tag{9}$$

$$CO_2 + M \rightleftharpoons CO_2^{\ddagger} + M \tag{10}$$

where $\ddagger$ denotes vibrational energy and the various species M are denoted in the following discussion as: $A \equiv N_2$, $B \equiv O_2$, $C \equiv O$, $D \equiv CO$, and $E \equiv CO_2$. The dominant V-V processes are:

$$N_2^{\ddagger} + CO \rightleftharpoons N_2 + CO^{\ddagger} \tag{11}$$

$$N_2^{\ddagger} + O_2 \rightleftharpoons N_2 + O_2^{\ddagger} \tag{12}$$

$$N_2^{\ddagger} + CO_2 \rightleftharpoons N_2 + CO_2^{\ddagger} \quad . \tag{13}$$

Because of their small relative concentrations, we will neglect V-V interactions between CO, O_2, and CO_2.

The equations governing the vibrational relaxation of gas mixtures were derived by Schwartz, Slawsky, and Herzfeld,[14] and they subsequently were put in a more convenient form by Taylor, Camac, and Feinberg.[12] In the latter form, the quantities Φ_i and X_i are defined, with $\Phi_i = (\bar{E}_i - E_i)/\bar{E}_i$ where E_i is the vibrational energy of species i at time t, $\bar{E}_i$ is the

equilibrium value, and X_i is the mole fraction of species i. The pertinent equations for this study, namely, for the relaxation of N_2 and CO, are:

$$-\frac{d\Phi_A}{dt} = \left[\frac{X_A}{\tau_{AA}} + \frac{X_B}{\tau_{AB}} + \frac{X_C}{\tau_{AC}} + \frac{X_D}{\tau_{AD}} + \frac{X_E}{\tau_{AE}}\right]\Phi_A$$

$$-\frac{X_B}{\tau_{AB}^v}\left[\frac{\Phi_B(1-\Phi_A)}{1-\exp(-\Theta_A)} - \frac{\Phi_A(1-\Phi_B)}{1-\exp(-\Theta_B)}\right]\cdot[1-\exp(-\Theta_A)]$$

$$-\frac{X_D}{\tau_{AD}^v}\left[\frac{\Phi_D(1-\Phi_A)}{1-\exp(-\Theta_A)} - \frac{\Phi_A(1-\Phi_D)}{1-\exp(-\Theta_D)}\right]\cdot[1-\exp(-\Theta_A)]$$

$$-\frac{X_E}{\tau_{AE}^v}\left[\frac{\Phi_E(1-\Phi_A)}{1-\exp(-\Theta_A)} - \frac{\Phi_A(1-\Phi_E)}{1-\exp(-\Theta_E)}\right]\cdot[1-\exp(-\Theta_A)] \quad (14)$$

and

$$-\frac{d\Phi_D}{dt} = \left[\frac{X_A}{\tau_{DA}} + \frac{X_B}{\tau_{DB}} + \frac{X_C}{\tau_{DC}} + \frac{X_D}{\tau_{DD}} + \frac{X_E}{\tau_{DE}}\right]\Phi_D$$

$$+\frac{X_A}{\tau_{AD}^v}\frac{\exp(\Theta_D)}{\exp(\Theta_A)}\left[\frac{\Phi_D(1-\Phi_A)}{1-\exp(-\Theta_A)} - \frac{\Phi_A(1-\Phi_D)}{1-\exp(-\Theta_D)}\right]\cdot[1-\exp(-\Theta_D)].$$

$$(15)$$

In these equations, $\Theta_i = h\nu_i/k$, τ_{ij} is the V-T relaxation time of species i infinitely dilute in species j, and τ_{ij}^v is the V-V relaxation time between species i and j. The first set of terms on the right hand side of these equations thus represents V-T relaxation, while subsequent terms represent V-V transfer with each of the possible collision partners. Note that in the case of V-V transfer between CO_2 and N_2, we restrict attention to the ν_3 mode of CO_2 $\left(\omega_e = 2349 \text{ cm}^{-1}\right)$.

Sato, et al., have solved a system of equations like (14) and (15) when there was only V-V exchange between two species.[13] In principle, a closed-form solution can also be obtained when there are additional V-V terms, but in practice, the algebra becomes unduly cumbersome. We will therefore neglect for the moment the V-V contributions of both O_2 and CO_2 and will show later that these terms are indeed negligible. We also assume at this point that $\Theta_A \cong \Theta_D$ and lump the coefficients of each of the V-T terms into a single parameter T_i^{-1}, where

$$\frac{1}{T_i} = \sum_j \frac{X_j}{\tau_{ij}} \quad .$$ (16)

The equations then simplify to

$$-\frac{d\Phi_A}{dt} = \left(\frac{1}{T_A} + \frac{X_D}{\tau_{AD}^v}\right) \Phi_A - \frac{X_D}{\tau_{AD}^v} \Phi_D$$ (14a)

and

$$-\frac{d\Phi_D}{dt} = -\frac{X_A}{\tau_{AD}^v} \Phi_A + \left(\frac{1}{T_D} + \frac{X_A}{\tau_{AD}^v}\right) \Phi_D \quad .$$ (15a)

The general solution of these equations was given by Sato, et al., as their equations (9) through (13),[13] and it need not be repeated here. When $X_A \gg X_B$ and $T_D \lesssim T_A$, the solutions simplify considerably and as given by Sato, et al., are:

$$\Phi_A = \exp(-t/T_A)$$ (17)

52

and

$$\Phi_D = \frac{1}{1+r} \exp[-(\frac{r+1}{T_D} - \frac{r}{T_A})t] + \frac{r}{1+r} \exp(-t/T_A) \quad , \qquad (18)$$

where

$$r = 1/[(T_D^{-1} - T_A^{-1}) \tau_{AD}^v] \quad . \qquad (19)$$

The solution $f \sim \Phi_A$ indicates that N_2 will relax with a single exponential risetime governed only by V-T processes, but that for Φ_D shows that CO will show a double exponential behavior as discussed in the previous section. When $\tau_{AD}^v \ll T_D$, r is large and the first term of equation (18) becomes negligible. This is normally the case in the IR tracer method.

Examination of equation (18) indicates that the initial time constant τ_1 observed in the relaxation profile is T_D, and that the final time constant τ_2 is T_A. Furthermore, the parameter r, which can be determined by extrapolating the final relaxation profile back to time zero, can be used in equation (19) to determine T_D once T_A is known, since τ_{AD}^v has already been determined by several investigators.[13,15,16] Since T_D can thus be determined in two ways, we have a means of checking on the internal consistency of the present results for τ_{CO-O}.

When $T_D \ll T_A$, the simplified solution above may not adequately account for V-V transfer from CO to N_2. In this case, the solution of Sato, et al., can be modified to give, instead of equations (17) and (18), the expressions:

$$\Phi_A = \exp\left[-\frac{1}{T_A}\left(1 + \frac{T_A}{T_D}\frac{X_D}{X_A}\frac{r}{1+r}\right)t\right] \qquad (20)$$

and

$$\Phi_D = \frac{1}{1+r}\exp\left[-\left(\frac{r+1}{T_D} - \frac{r}{T_A}\right)t\right] +$$

$$\frac{r}{1+r}\exp\left[-\frac{1}{T_A}\left(1 + \frac{T_A}{T_D}\frac{X_D}{X_A}\frac{r}{1+r}\right)t\right] . \qquad (21)$$

Since $(r/1+r) < 1$ and $(X_D/X_A) = 0.01$, we see from equation (20) that V-V transfer from CO to N_2 becomes important when $T_D \lesssim 0.1\ T_A$. We find from measurements of $p\tau_{CO-O}$ and from calculations that the differences between T_D and T_A are in some cases greater than this, and, therefore, we use these more complete equations to calculate the rate of relaxation of N_2 in this study.

Equation (20) can also be used to examine the effects of O_2 and CO_2 on the relaxation of N_2. We have already made the assumption that each of these species relaxes by V-T processes or by V-V interaction only with N_2. In each case, then, the effect of species i on N_2 will be negligible if

$$R_i \equiv \frac{X_i}{X_A}\frac{T_A}{T_i}\frac{r}{1+r} \leq \frac{X_i}{X_A}\frac{T_A}{T_i + \tau_{Ai}^v} \ll 1 . \qquad (22)$$

We can calculate T_{O_2}, including the effects of O atoms, from the results of Kiefer and Lutz,[1] and $\tau_{N_2-O_2}^v$ from the results of White[9] and Kamimoto and Matsui.[10] In this case, the V-V transfer is relatively slow $(r \ll 1)$,

and since $X_{O_2} \leq 0.015$, we find $R_{O_2} < 0.05$. For CO_2, preliminary informa-
tion on the relaxation of CO_2 by O atoms indicates that process to be
negligible here.[17] The relaxation times T_{CO_2} and $\tau^v_{N_2-CO_2}$ can then be ob-
tained, for example, from the results of Taylor and Bitterman.[18] Taking
the maximum concentration of CO_2 as $X_{CO_2} \leq 0.001$ then gives $R_{CO_2} < 0.08$.
Therefore, within the accuracy inherent in this study, the effects of O_2
and CO_2 can safely be neglected.

Having related τ_1 and τ_2 to T_D and T_A through equation (21), we can
proceed to find τ_{N_2-O} and τ_{CO-O}. From equation (16), we have

$$\frac{1}{T_A} = \frac{X_{N_2}}{\tau_{N_2-N_2}} + \frac{X_{O_2}}{\tau_{N_2-O_2}} + \frac{X_O}{\tau_{N_2-O}} + \frac{X_{CO}}{\tau_{N_2-CO}} + \frac{X_{CO_2}}{\tau_{N_2-CO_2}} \quad (23)$$

and

$$\frac{1}{T_D} = \frac{X_{N_2}}{\tau_{CO-N_2}} + \frac{X_{O_2}}{\tau_{CO-N_2}} + \frac{X_O}{\tau_{CO-O}} + \frac{X_{CO}}{\tau_{CO-CO}} + \frac{X_{CO_2}}{\tau_{CO-CO_2}} \quad (24)$$

However, on the basis of Millikan and White's correlation,[6] for example,
we assume $\tau_{N_2-O_2}$, τ_{N_2-CO}, and $\tau_{N_2-CO_2}$ approximately equal to $\tau_{N_2-N_2}$,
and likewise τ_{CO-N_2}, τ_{CO-O_2}, and τ_{CO-CO_2} equal to τ_{CO-CO}. Then, since
$X_O \leq 0.01$ so that $X_{N_2} + X_{O_2} + X_{CO} + X_{CO_2} \cong 1$, we obtain the expressions

$$\tau_{N_2-O} = \frac{X_O \cdot \tau_{N_2-N_2} \cdot T_A}{\tau_{N_2-N_2} - T_A} \quad (25)$$

B-17

and

$$\tau_{CO-O} = \frac{X_O \cdot \tau_{CO-CO} \cdot T_D}{\tau_{CO-CO} - T_D}. \qquad (26)$$

The times $\tau_{N_2-N_2}$ are taken from the curve of Figure 1, and the τ_{CO-CO}'s are taken from the results of Hooker and Millikan.[19]

In analyzing the data, thermodynamic properties behind the shock-wave were calculated for the gas mixture, pressure, and Mach number of each test. The fraction of O_3 converted to O atoms was also calculated, using the method described in the Appendix. Results for each test are presented for a temperature that is an average between the values calculated for vibration frozen and for full vibrational equilibrium, with the O_3 assumed dissociated in both cases. The maximum difference between these two temperatures is approximately 12%.

V RESULTS

In view of the possible contribution of V-V transfer from CO to the relaxation of N_2 as indicated in equations (20) and (21), we report first our measured relaxation times $p\tau_{CO-O}$. The results derived from the Ar-1% CO-1% O_3 measurements, presented in Figure 4, indicate that $p\tau_{CO-O}$ is approximately 0.04 atm-μs. Although limited in number, these values are in good agreement with the more extensive measurements of Center, which were obtained by using similar gas mixtures.[17] Unfortunately, the results for $p\tau_{CO-O}$ obtained from the N_2-CO-O_3 tests are neither consistent nor readily explainable. As discussed above, $p\tau_{CO-O}$ can be determined both from the initial risetime and from the intercept parameter r. The results based on the initial risetime τ_D are on the order of ten times longer than those presented in Figure 4, while those based on the parameter r range from 1/10 to 1/4 as long as those of Figure 4. From these anomalies, the conclusion is that neither the initial risetime nor the intercept are solely related to the CO-O relaxation process; hence for the time being, this interesting effect must await an alternative explanation.

Because of the uncertain interpretation of the initial risetime, we calculate the relaxation time of CO in the N_2-CO-O_3 mixture using the results for τ_{CO-O} from Figure 4. The relaxation times $p\tau_{N_2-O}$ for N_2 by O atoms are then determined from equations (21) and (25), and the results are presented in Figure 5 for each of the nominal O_3 concentrations. Including the uncertainties of the measurements of the physical quantities ($\pm$ 20%), of the correction for V-V transfer from CO and of possible contributions from other minor species or impurities, the total uncertainty of these results is estimated to be $\pm$ 50%

Also shown in Figure 5 are the earlier results of Breshears and Bird,[2] the low temperature results of McNeal, et al.,[5] and the predictions

B-19
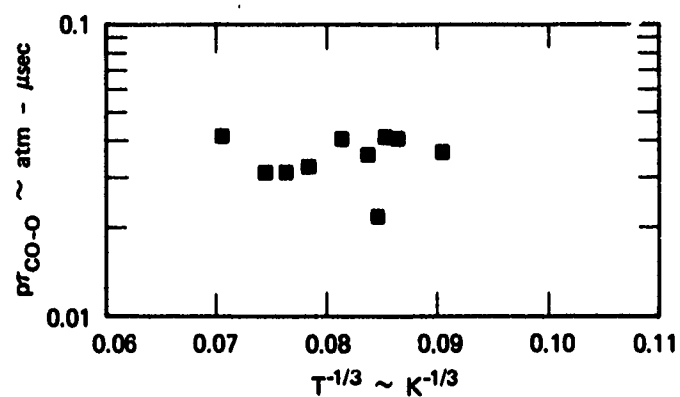
FIGURE 4   RELAXATION TIMES FOR THE VIBRATIONAL
            RELAXATION OF CO BY OXYGEN ATOMS
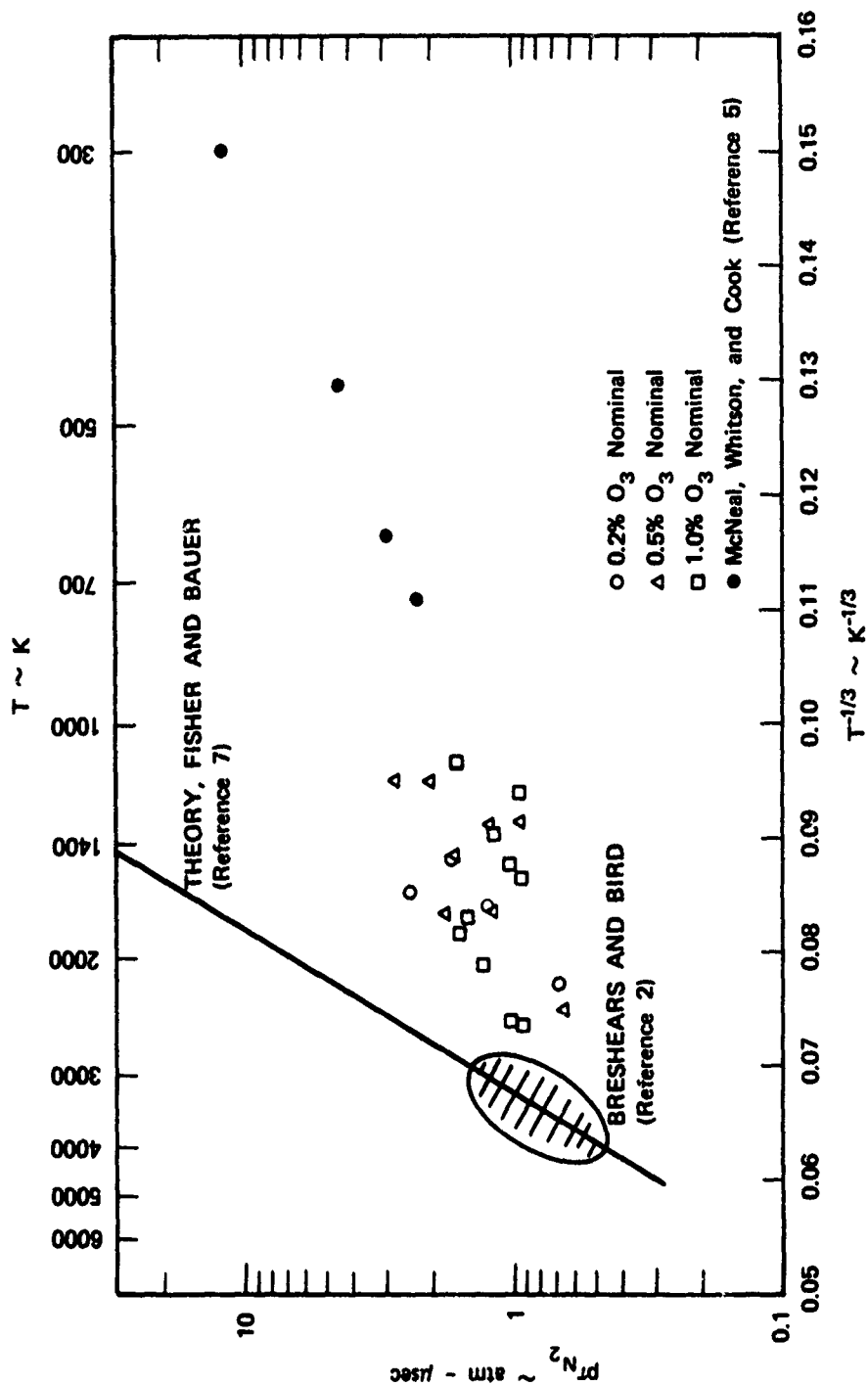
FIGURE 5   RELAXATION TIMES FOR THE VIBRATIONAL RELAXATION OF N_2 BY OXYGEN ATOMS

SA-1664-13

B-21

of Fisher and Bauer.[7] Although the data show substantial scatter, the current results agree very well in magnitude with both the earlier shock tube results and with the low-temperature results.

As noted earlier, a very large disagreement exists between the temperature-dependences of the theoretical and experimental results. In the theoretical prediction, the temperature-dependence results from a specification of the height of the crossing point of the $N_2 + O(^3P)$ and the $N_2 + O(^1D)$ potential curves above the asymptotic limit of the $N_2 + O(^3P)$ curve. Fisher and Bauer used a value of 0.8 eV for this barrier height or "activation energy" based on the unimolecular decomposition of N_2O.[7] If their model is to apply, the activation energy must actually be less than 0.2 eV, although the theoretical curve does not fit the shape of the experimental data very well even under that assumption. The activation energy could differ from the deduced value of 0.8 eV because of vibrational excitation effects in the N_2O dissociation or because of orientation effects in the $O-N_2$ interaction.[7] It is clear that additional work is required to provide an adequate theoretical explanation of these rapid relaxation rates.

VI CONCLUSIONS

The results presented here for the rate of relaxation of N_2 by O atoms are important in that they serve to substantiate both the existing high- and low-temperature results. In particular, with this verification of the low-temperature results, the observed vibrational temperature of N_2 in the upper atmosphere can now be explained.[20,21] The pronounced difference between the observed and predicted temperature-dependence of this relaxation rate also presents a challenge to find an adequate theoretical understanding of this process.

The relaxation rate for CO by O atoms determined from tests in Ar-CO-O_3 mixtures is in good agreement with other recent measurements. This rate is approximately 25 times as fast as the N_2-O rate and, coincidentally, is approximately the same as that for the relaxation of O_2 by O atoms. The greater rapidity of the CO-O and O_2-O relaxation, compared with that of N_2-O, may be the result of atom-exchange processes in the former cases.
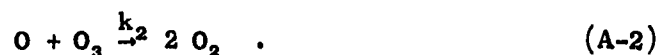
ACKNOWLEDGEMENTS

Appendix

DECOMPOSITION OF SHOCK-HEATED OZONE

The decomposition of shock-heated O_3 and its conversion to O and O_2 is governed by the reactions:

$$O_3 + M \xrightarrow{k_1} O + O_2 + M \qquad (A-1)$$

and

$$O + O_3 \xrightarrow{k_2} 2\,O_2 \quad . \qquad (A-2)$$

Wray[22] has shown that, at the completion of the decomposition process, the mole fraction of O atoms (X_O) and of initial $O_3 (X_{O_3})$ are related by

$$X_O = (1-\beta)\, X_{O_3} \quad , \qquad (A-3)$$

where β is given by the solution of the equation

$$\ln\,[1-G(1-\beta)] + \tfrac{1}{2}\,G(1-\beta) + \tfrac{1}{2}\,G = 0 \quad . \qquad (A-4)$$

The parameter G is related to X_{O_3} and the reaction rates k_1 and k_2 by

$$G = X_{O_3}\,(k_2/k_1) \quad . \qquad (A-5)$$

It can be shown that β is asymptotic to G for $G \ll 1$ and to $1-1/G$ for $G \gg 1$. With this information and some numerical solutions of equation (A-4), the variation of β with G for all values of G has been determined and is presented in Figure A-1. As noted earlier, for high temperatures where $k_2/k_1 \cong 1$ and for $X_{O_3} \ll 1$, $\beta \to G \to 0$ and there is a one-to-one conversion of O_3 to O atoms. Conversely, for low temperatures

B-24
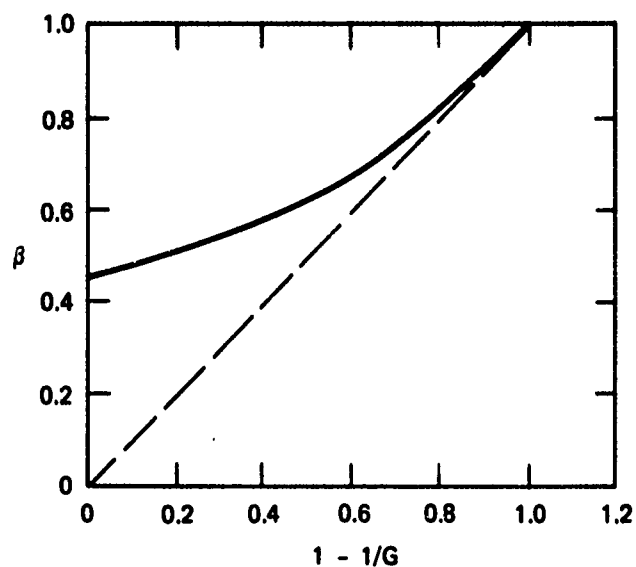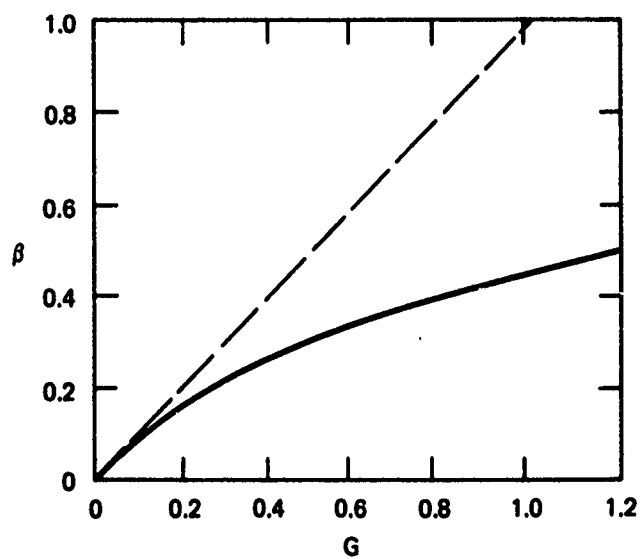

SA-1684-7

FIGURE A-1   THE OZONE DISSOCIATION PARAMETER
             β VERSUS THE PARAMETERS G AND 1 - 1/G

$$(\beta = 1 - X_O/X_{O_3}, \quad G = X_{O_3} \cdot k_2/k_1)$$

where $k_2/k_1 \gg 1$, G may be much larger than 1 so that $\beta \to 1$. Then there are very few O atoms produced.

The decomposition of O_3 has been studied by Jones and Davidson[23] (JD), Myers and Bartle[24] (MB), Benson and Axworthy[25] (BA), and Michael.[26] They have given the following rate equations, in units of liter/mole-s:

(JDI) : $\quad k_1 = 5.8 \times 10^{11} \exp(-23,500/RT)$

(JDII) : $\quad k_1 = 3.4 \times 10^{8} T^{\frac{1}{2}} (24,350/RT)^{1.75} \exp(-24350/RT)$

(JD) : $\quad k_2 = 2.4 \times 10^{10} \exp(-5,600/RT)$

(MB) : $\quad k_2 = 1.04 \times 10^{9} T^{\frac{1}{2}} \exp(-5,288/RT)$

(BA) : $\quad k_2 = 3.37 \times 10^{10} \exp(-5,700/RT)$.

The magnitudes of these rates are such that the largest ratio of k_2/k_1 is formed from the combination $k_2(MB)/k_1(JDII)$ while the smallest ratio is formed from $k_2(JD)/k_1(JDI)$, as shown in Figure A-2. The latter ratio, based on data in the 680-920 K temperature range, has been the standard of comparison for most studies involving O_3 decomposition in the shock tube, and most investigators have found that k_2/k_1 exceeds the JD extrapolation by an increasing amount as the temperature increases. For example, Michael reports a factor of 2.5 at 1300 K,[26] Wray estimates a factor of 10 for 1300 to 2900 K,[22] and Kiefer and Lutz estimate values of 3 to 30 for 1500 to 3000 K.[1,27] The combination $k_2(MB)/k_1(JDII)$ comes close to giving the observed ratio for all temperatures, but there is little theoretical justification for those rates. Rather, it is more likely that k_2 is well represented by the JD or BA expressions while k_1 deviates from all of the given expressions as temperature increases. In this work, therefore, we have chosen to use the $k_2(BA)$ rate, together with $k_1(JDI)$ modified downward by a factor $(900/T)^2$, which gives agreement with the empirical observations. The ratio resulting from this combination is also given in Figure A-2.
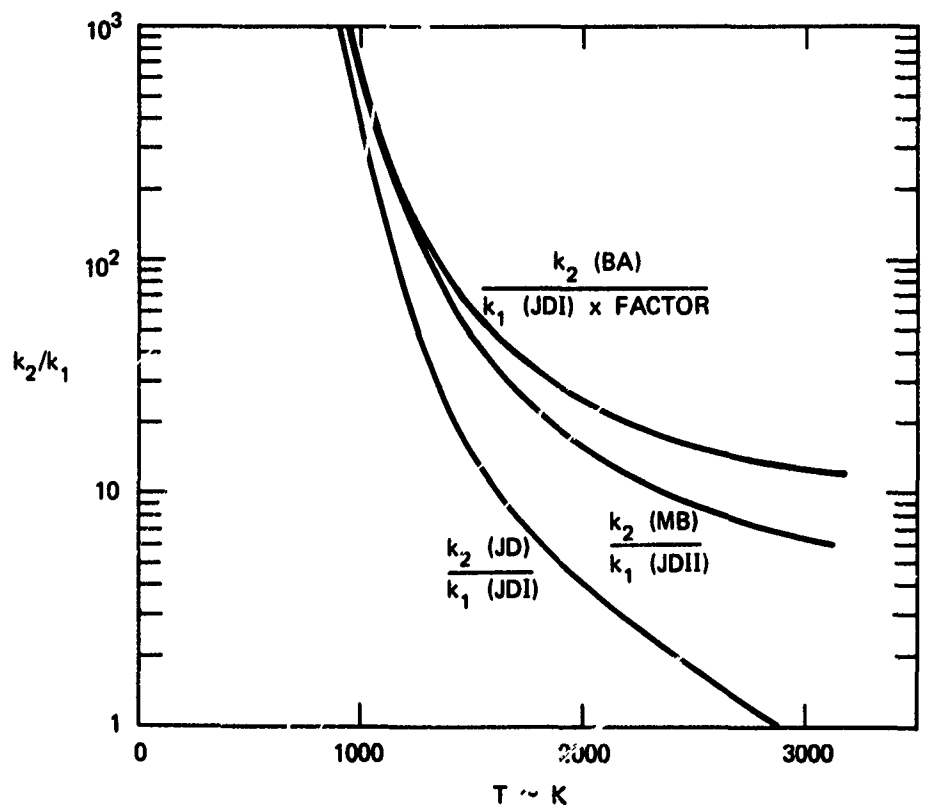
FIGURE A-2   VARIOUS COMBINATIONS OF RATE CONSTANTS
FOR OZONE DECOMPOSITION

(See text for definitions.)

B-27

The fractional decomposition of O_3 into O atoms determined from equation (A-4) and the various ratios k_2/k_1 of Figure A-2 is given in Figure A-3 for the cases $X_{O_3} = 0.002$ and 0.01. In the case of $X_{O_3} = .002$, the differences resulting from the extreme choices of k_2/k_1 range from 20% at 1000 K to 5% for T > 2000, while for $X_{O_3} = .01$ the differences range from 45% at 1000 K to 15% at 2000 K. The results using the empirical ratio of k_2/k_1 are regarded as a best estimate of X_O/X_{O_3}, and the uncertainty is probably somewhat less than the maximum difference obtained using the limiting ratios of k_2/k_1.
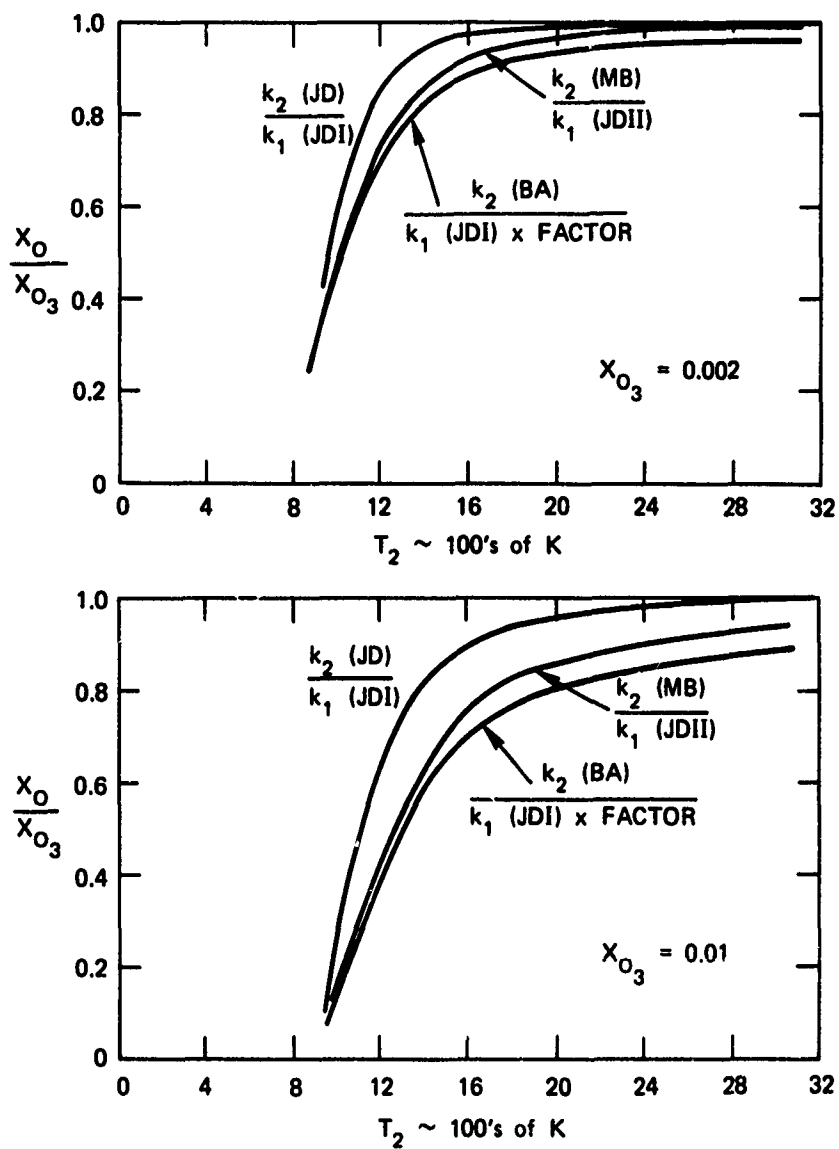
FIGURE A-3   FRACTIONAL PRODUCTION OF OXYGEN ATOMS
FROM OZONE AS FUNCTION OF TEMPERATURE,
INITIAL CONCENTRATION OF OZONE, AND
CHOICE OF RATE CONSTANTS

B-29

REFERENCES

1. J. H. Kiefer and R. W. Lutz, Eleventh Symp. (Int.) on Combustion, The Combustion Institute, Pittsburgh, 1967.

2. W. D. Breshears and P. F. Bird, J. Chem. Phys. 48, 4768 (1968).

3. C. W. von Rosenberg, Jr., R. L. Taylor and J. D. Teare, J. Chem. Phys. 54, 1974 (1971); J. Chem. Phys. 48, 5731 (1968).

4. C. W. von Rosenberg, Jr., and K. L. Wray, Eighth Int. Shock Tube Symp., London, July 1971; J. Chem. Phys. 54, 1406 (1971).

5. R. J. McNeal, M. E. Whitson, Jr., and G. R. Cook, Chem. Phys. Letters 16, 507 (1972); Trans. Amer. Geophys. Union (to be published).

6. R. C. Millikan and D. R. White, J. Chem. Phys. 39, 3209 (1963).

7. E. R. Fisher and E. Bauer, J. Chem. Phys. 57, 1966 (1972).

8. R. C. Millikan and D. R. White, J. Chem. Phys. 39, 98 (1963).

9. D. R. White, J. Chem. Phys. 49, 5472 (1968).

10. G. Kamimoto and H. Matsui, AIAA J. 7, 2358 (1969).

11. R. C. Millikan, J. Chem. Phys. 38, 2855 (1963).

12. R. L. Taylor, M. Camac, and R. M. Feinberg, Eleventh Symp. (Int.) on Combustion, The Combustion Institute, Pittsburgh, 1967.

13. Y. Sato, S. Tsuchiya, and K. Kuratani, J. Chem. Phys. 50, 1911 (1969).

14. R. N. Schwartz, Z. I. Slawsky, and K. F. Herzfeld, J. Chem. Phys. 20, 1591 (1952).

15. T. I. McLaren and J. P. Appleton, Eighth Int. Shock Tube Symp., London, 1971.

16. C. W. von Rosenberg, Jr., K. N. C. Bray, and N. H. Pratt, J. Chem. Phys. 56, 3231 (1972).

17. R. E. Center, AVCO-Everett Research Laboratory, private communication.

18. R. L. Taylor and S. Bitterman, J. Chem. Phys. 50, 1720 (1969).

19. W. J. Hooker and R. C. Millikan, J. Chem. Phys. 38, 214 (1963).

20. E. L. Breig, M. E. Brennan, and R. J. McNeal, J. Geophys. Res. (1973), to be published.

21. E. Jamshidi, E. R. Fisher, and R. H. Kummler, J. Geophys. Res. (1973), to be published.

22. K. L. Wray, J. Chem. Phys. 38, 1518 (1963).

23. W. M. Jones and N. Davidson, J. Am. Chem. Soc. 84, 2868 (1962).

24. B. F. Myers and E. R. Bartle, J. Chem. Phys. 48, 3935 (1968).

25. S. W. Benson and A. E. Axworthy, J. Chem. Phys. 42, 2614 (1965).

26. J. V. Michael, J. Chem. Phys. 54, 4455 (1971).

27. J. H. Kiefer and R. W. Lutz, J. Chem. Phys. 42, 1709 (1965).